communications biology

Article

A Nature Portfolio journal

https://doi.org/10.1038/s42003-025-09478-7

Engineering bidirectional chloroplast promoters for tunable co-expression of multiple genes in microalgae (*Chlamydomonas reinhardtii*)

Arnold William Tazon, Natacha Mérindol, Elisa Fantino, Ayoub Bouhadada, Fatima Awwad, Fatma Meddeb-Mouelhi & Isabel Desgagné-Penix

Chloroplasts offer significant potential for multigene engineering in microalgae, but the lack of well-characterized regulatory elements and limited understanding of plastid transcriptional mechanisms have hindered progress. Here, through a comparative conservation analysis across fifteen species of microalgae and higher plants, we identified bidirectional promoter (BDP) intergenic regions (IRs) showing diverse evolutionary trajectories, from lineage-specific rearrangements of *atpA/rbcL* (BDP1) and *chlL/petB* (BDP2), to strict conservation of the *psbH/psbN* IR (BDP3), and complete loss of *rpoB-1/psbF* (BDP4). Based on promoter signature analysis, we selected three candidate regions (BDP1, BDP2, and BDP3) from the *Chlamydomonas reinhardtii* chloroplast genome for functional characterization. A semi-rational screen revealed that BDP1 supports expression of two transgenes, *mVenus* and *tdTomato* in opposing orientations; BDP2 drives balanced expression, but low protein accumulation; and BDP3 exhibits minimal activity, suggesting UTR-dependent post-transcriptional regulation. Strikingly, methyl-jasmonate selectively enhanced *tdTomato* expression from BDP1, offering a chemical method to regulate chloroplast transgene expression. Collectively, these results underscore the evolutionary diversity and functional potential of natural BDPs, particularly BDP1, as powerful tools for multigene engineering and chemical modulation in microalgae and higher plants. This study also provides fundamental insights into chloroplast transcription, establishing a basis for future investigations into its regulatory mechanisms.

The use of microalgae in synthetic biology has expanded rapidly in recent decades, driven by their fast growth, cost-effective cultivation, and ability to capture industrial CO_2 emissions[1,2]. Moreover, green microalgae are generally recognized as safe by the United States Food and Drug Administration, mitigating concerns about environmental contamination during large-scale cultivation[3,4]. *Chlamydomonas reinhardtii* has emerged as a key model organism for biotechnological applications, particularly in biomass production, recombinant protein synthesis, plant-specialized metabolite biosynthesis, and biofilm formation. This versatility stems from its well-established transformation techniques, enabling precise genetic control across its three genomes (nuclear, mitochondrial, and chloroplast)[5]. Although commonly employed, transgene insertion into nuclear DNA is random and often results in gene silencing[6]. In contrast, chloroplast genome transformation offers several advantages: (i) precise transgene integration via homologous recombination, (ii) absence of transgene silencing mechanisms, (iii) high recombinant protein yields (up to 20% of total soluble proteins), (iv) stable integration of multiple transgene copies due to the polyploid nature of the chloroplast, and (v) abundant natural substrates for genetic engineering[7–9].

To fully harness the potential of *C. reinhardtii* chloroplasts, significant efforts have been directed toward achieving robust expression of multiple transgenes. Larrea-Alvarez and Purton[10] successfully demonstrated the simultaneous accumulation of four exogenous proteins by integrating expression cassettes into two distinct loci through iterative transformations.

Department of Biochemistry, Chemistry, Physics and Forensic Science, Université du Québec à Trois-Rivières, Trois-Rivières, QC, Canada.
e-mail: Isabel.Desgagne-Penix@uqtr.ca

However, this approach primarily relied on diverse 5' untranslated region (UTR) regulatory elements derived from endogenous chloroplast genes, which are not always optimal for driving high-level transgene expression[11]. Inspired by the prokaryotic ancestry of the plastid, polycistronic operon strategies have also been used to facilitate multigene expression within the *C. reinhardtii* chloroplast. Macedo-Osorio, et al.[12] successfully co-expressed aminoglycoside 3'-phosphotransferase and green fluorescent protein (GFP) from a bicistronic mRNA using long inter-cistronic sequences derived from the endogenous chloroplast genome. To reduce the size of polycistronic mRNA constructs, shorter inter-cistronic elements (55 and 47 bp) from *Nicotiana tabacum* (*rps19*/*rpl22*) and *Synechococcus elongatus* (*apcA*/*apcB*) were later employed to construct bicistronic or tricistronic operons in *C. reinhardtii* chloroplast[11]. However, in these systems, transgenes located in downstream positions within the operon often exhibited reduced or inconsistent expression levels. Similarly, positional effects have been reported by Guo, et al.[13] coexpressing *cbbL*, encoding the Rubisco large subunit from *Thiobacillus neapolitanus*, and *Nluc*, encoding NanoLuc luciferase, from a bicistronic operon in the chloroplast of *C. reinhardtii*. The gene in the second position consistently showed poor expression, highlighting a recurring limitation in chloroplast operon design. Overcoming these challenges is essential to unlock the chloroplast and further expand its applications in synthetic biology[14]. Collectively, these studies emphasize the need to develop advanced molecular tools and regulatory elements tailored to the chloroplast transcriptional and translational machinery. In line with this, recent work has introduced a high-throughput chloroplast engineering framework in *C. reinhardtii*, expanding standardized regulatory parts and demonstrating the feasibility of rapid prototyping of synthetic pathways within the plastid[15].

Promoter structure refers to the organization of specific sequence motifs, such as the TATA-box; CAAT-box; -35 and -10 elements, that collectively regulate the initiation and strength of transcription[16,17]. In *C. reinhardtii*, both nuclear and chloroplast promoters have been extensively studied: nuclear promoters often contain canonical eukaryotic elements like the TATA-box and CAAT-box, whereas chloroplast promoters, reflecting their prokaryotic ancestry, typically rely on bacterial-like -35 and -10 motifs recognized by plastid-encoded RNA polymerases (PEP) or YRTA motif recognized by nuclear-encoded RNA polymerases (NEP)[18–20]. A variety of endogenous promoters have been characterized in chloroplasts, including those from *psbA*[21,22], *atpA*[23], *psbD*[24,25], and *rbcL*[26], each exhibiting different transcriptional strengths and regulatory behaviors. Between the promoter and the initiation codon, and between the stop codon and the terminator, transcripts include 5′ or 3′ UTRs subjected to post-transcriptional processes, which play a pivotal role in determining gene expression outcomes in the chloroplast. These include RNA processing (cleavage of polycistronic transcripts) and, particularly, mRNA stability and translation regulation. A large part of this regulation is mediated by nucleus-encoded trans-acting factors (NTAFs) that are imported into the organelle and act in a sequence-specific manner. These proteins bind to the 5′ or 3′ UTRs of chloroplast mRNAs to enhance their stability or promote translation. For instance, MDA1 and TDA1 are essential for the stabilization and translation of *atpA* transcripts[27], while NAC2, MRL1, MCA1, and MBB1 are required for the accumulation of *psbD*, *rbcL*, *petA*, and *psbB/psbH* transcripts, respectively[28–32]. Additionally, treatment of *C. reinhardtii* with methyl jasmonate (MeJA) was reported to induce the upregulation of nuclear genes encoding key enzymes of the chloroplast-localized 2-C-methyl-D-erythritol 4-phosphate (MEP) pathway[33]. This intricate nuclear-plastid communication network enables the nucleus to exert tight post-transcriptional control over chloroplast gene expression, ensuring the proper coordination of plastid functions with cellular developmental programs and environmental cues.

Understanding the diversity and the native structural organization of these promoter elements is essential for elucidating chloroplast transcriptional regulation, optimizing transgene expression, and enabling the rational design of robust multigene expression systems. Through bioinformatic and genetic engineering approaches, various intergenic regions (IRs) located between head-to-head (h2h) genes have been identified and characterized as active natural bidirectional promoters (BDPs) in plants, including *Arabidopsis thaliana*, *Capsicum annuum*, *Oryza sativa*, and *Zea mays*[34–37]. BDPs are short regulatory DNA sequences, typically ≤ 1000 bp, that separate and drive the transcription of adjacent genes oriented on opposite DNA strands[38]. Functional characterization of BDPs across bacteria, yeasts, and plants has demonstrated their ability to coordinate multiple genes' expression, enhance heterologous protein accumulation, and improve protein stability, particularly in complex metabolic pathways[34,38–40]. Recently, Poliner, et al.[41] developed a high-capacity gene stacking toolkit for the bidirectional expression of recombinant proteins in the nuclear genome of the microalga *Nannochloropsis oceanica*, illustrating the potential of BDPs for orchestrating multi-gene expression in algal systems.

Despite these advancements, the systematic identification and functional validation of naturally active BDPs in the chloroplast genome of the model green microalga *C. reinhardtii* remain unexplored. Establishing endogenous chloroplast BDPs could significantly expand this organism's synthetic biology toolkit for multigene expression while shedding light on chloroplast transcriptional regulation, including promoter architecture, transcription factor interactions, and RNA stability. In this study, we present the development of advanced molecular tools based on a BDP engineering strategy, leveraging a semi-rational screening of IRs between divergent gene pairs in the *C. reinhardtii* chloroplast genome. Using a comparative conservation analysis across fifteen species of microalgae and higher plants, a combination of quantitative RT-qPCR, flow cytometry, immunoblotting, and confocal microscopy, we selected BDPs and demonstrate that co-expression of heterologous proteins from bidirectional mRNA in the chloroplast of *C. reinhardtii* is not only feasible but also opens transformative possibilities for chloroplast multigene engineering. To the best of our knowledge, this study is the first to systematically characterize native BDPs for transgene expression in any chloroplast system. These findings provide a foundational resource for chloroplast multigene engineering and provide insights into bidirectional transcriptional and chemical regulation in algal plastids.

Results

Architecture and evolutionary conservation of bidirectional promoters from four head-to-head gene pairs in the *C. reinhardtii* chloroplast

The structural organization of *C. reinhardtii* chloroplast genes was analyzed through in silico curation and visualization of available annotations (GenBank accession: FJ423446.1) using NCBI Genome Data Viewer (GDV). This analysis focused on divergently transcribed gene pairs separated by potential BDP IRs. Four gene pairs exhibiting a h2h structural organization were identified: BDP1 *atpA/rbcL* (nucleotides 124,142–125,000), BDP2 *chlL/petB* (nucleotides 20,688–21,321), BDP3 *psbN/psbH* (nucleotides 77,156–77,725), and BDP4 *rpoB-1/psbF* (nucleotides 101,307–102,362). These four BDP-associated IRs were subsequently analyzed to determine the type and structural features of their promoters. In *C. reinhardtii*, PEP-dependent promoters typically resemble canonical bacterial σ^{70}-type promoters, characterized by conserved −10 (TATAAT) and −35 (TTGACA) motifs[19,20]. Prior studies have shown that the -10 region within *C. reinhardtii* chloroplast promoters frequently expands into an octameric palindromic motif (TATAATAT), a distinctive hallmark of plastid transcriptional regulation[20]. To elucidate the intrinsic promoter architecture of the BDPs in the absence of their associated 5′ UTRs[23,42–46] (Supplementary Table 1), we combined a manual strand-specific search with computational promoter prediction using BPROM[47]. This tool predicts bacterial-type promoters by identifying -10 and -35 elements and calculating their similarity to canonical consensus sequences, along with a confidence score for promoter functionality. Promoter mapping revealed distinct structural features within each BDP. In BDP1, the reverse orientation contained a −10 motif (ATATATAAT) and a variant −35 motif (TTTACA) located at −68 and −94 bp upstream of the *rbcL* transcription start site (*TSS*), while the forward orientation displayed −10 and −35 motifs at −44 and −69 bp relative to the

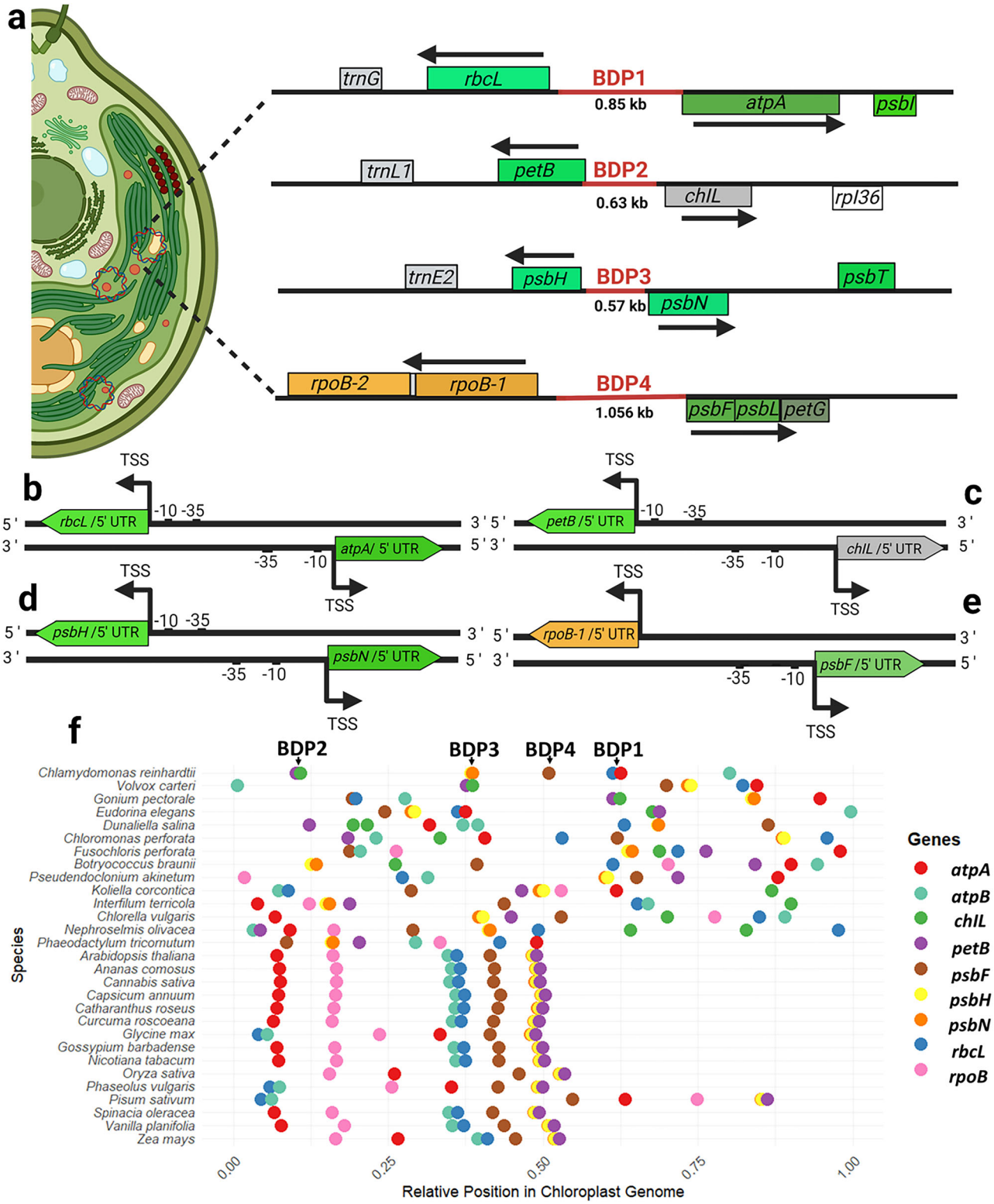

atpA TSS (Fig. 1b; Table 1 and Supplementary Fig. 1a). In BDP2, the reverse strand carried −10 and −30 elements positioned at −27 and −55 bp from *petB*, whereas the forward strand showed a − 10 motif at −225 and a − 35 motif at −247 bp upstream of *chlL* (Fig. 1c; Table 1 and Supplementary Fig. 1b). Similarly, BDP3 contained a − 10 and a − 35 element at −34 and −60 bp relative to *psbH* in the reverse orientation, and at −194 and −218 bp on the forward strand relative to *psbN* (Fig. 1d; Table 1 and Supplementary Fig. 1c). In BDP4, only the forward orientation displayed promoter motifs, with a − 10 and −35 element located 104 and 127 bp upstream of *psbF* (Fig. 1e; Table 1 and Supplementary Fig. 1d). Across nearly all BDPs, the −35 elements began with TTG/TTT, in agreement with previous chloroplast RNA-seq analyses. This analysis confirmed that the candidate IRs of BDP1-3 display the sequence characteristics of bidirectional promoters.

The specific gene pairs proposed to be controlled by the candidate BDPs in *C. reinhardtii* were used in a comparative analysis of chloroplast

Fig. 1 | Genomic context and promoter architecture of bidirectional promoter regions in the chloroplast genome. a Schematic representation of the *C. reinhardtii* chloroplast highlighting the genomic positions of four divergent gene pairs arranged in a head-to-head (h2h) orientation: *rbcL/atpA* (BDP1), *petB/chlL* (BDP2), *psbH/psbN* (BDP3), and *rpoB-1/psbF* (BDP4). The intergenic regions separating each gene pair are designated as BDP1–BDP4 (in red) and were identified as candidate endogenous bidirectional promoters. Arrows indicate the transcriptional orientation of each gene. Gene box sizes are proportional to gene length, and coding sequences (CDS) are color-coded by operon or gene identity. **b–e** Core promoter architecture of BDP1 to BDP4 IRs, showing canonical prokaryotic-like promoter motifs on both DNA strands. Conserved −10 (TATAATAT or variant) and −35 (TTGACA or variant) elements were annotated based on proximity to the transcription start sites (TSSs) of each gene using a combination of manual strand-specific searches and computational promoter prediction with BPROM (Softberry Inc., Mount Kisco, NY, USA; http://linux1.softberry.com). The 5′ untranslated regions (5′ UTRs) are also indicated. **f** Evolutionary conservation of BDP1–4 bidirectional promoters in microalgae and higher plants. Distribution of nine target genes (*atpA, atpB, chlL, petB, psbF, psbN, psbH, rbcL*, and *rpoB*) along the chloroplast genomes of 28 species (Supplementary Table 2), including microalgae (top) and higher plants (bottom). Each dot represents the normalized relative position of genes flanking BDP1–4 within the chloroplast genome, illustrating conserved bidirectional promoter arrangements across photosynthetic microalgae and higher plants. Species are ordered by phylogenetic grouping, and colors correspond to specific flanking genes as indicated in the legend. Microalgae (chloroplast genome size) : *C. reinhardtii* (205 kb); *F. perforata* (149 kb); *B. braunii* (156 kb); *P. akinetum* (195 kb); *K. corcontica* (205 kb); *I. terricola* (222 kb); *C. vulgaris* (150 kb); *N. olivacea* (200 kb); *C. perforata* (195 kb); *V. carteri* (137 kb); *D. salina* (269 kb); *H. pluvialis* (135 kb); *G. pectorale* (223 kb); *E. elegans* (222 kb); *P. tricornutum* (117 kb). higher plants (chloroplast genome size): *A. comosus* (159 kb); *C. sativa* (153 kb); *C. annuum* (156 kb); *C. roseus* (154 kb); *C. roscoeana* (162 kb); *G. max* (152 kb); *G. barbadense* (160 kb); *N. tabacum* (156 kb); *O. sativa* (134 kb); *P. vulgaris* (150 kb); *P. sativum* (122 kb); *S. oleracea* (150 kb); *V. planifolia* (152 kb); *Z. mays* (140 kb); *A. thaliana* (154 kb).

Table 1 | Predicted chloroplast promoter elements within bidirectional promoter candidates

Intergenics regions	-35 box (pos; seq; score)	-10 box (pos; seq; score)	LDF score
$_{atpA}$*BDP1*	-69; TTTATA; 39	-44; TGCTATAAT; 88	11.12
BDP1$_{rbcL}$	-94; TTTACA; 47	-68; ATATATAAT; 70	11.47
$_{petB}$*BDP2*	-55; TTGTAT; 42	-27; TACTAACGT; 25	11.28
BDP2$_{chlL}$	-247; AGGACA; -1	-225; TGGTACAAT; 78	7.30
$_{psbN}$*BDP3*	-218; TTGTTA; 45	-194; ATTTTTAAT; 43	11.79
BDP3$_{psbH}$	-60; TTTCCT; 37	-34; AAATAAAAT; 56	7.44
$_{psbF}$*BDP4*	-127; TTTCAA; 36	-104; ATTTAACAT; 56	12.16

For each predicted promoter, the table lists the promoter position relative to the intergenic sequence, the positions, sequences, and scores of the -35 and -10 boxes, and the Linear Discriminant Function (LDF) score from the prediction algorithm. Positions are given in base pairs relative to the intergenic region sequence. Scores indicate motif similarity to the consensus sequence, and higher LDF values denote stronger promoter likelihood above the detection threshold. LDF between 3–6, possible promoter (requires experimental confirmation); LDF between 6–9, probable promoter (good consistency of −10/ − 35 motifs and spacing); LDF > 9, very probable promoter (strong match with σ^{70}-type promoter features).

gene organization among microalgae (including *Fusochloris perforata, Botryococcus braunii, Pseudendoclonium akinetum, Koliella corcontica, Interfilum terricola, Chlorella vulgaris, Nephroselmis olivacea, Chloromonas perforata, Volvox carteri, Dunaliella salina, Gonium pectorale, Eudorina elegans* and *Phaeodactylum tricornutum*) and higher plants (*Arabidopsis thaliana, Ananas comosus, Cannabis sativa, Capsicum annuum, Catharanthus roseus, Curcuma roscoeana, Glycine max, Gossypium barbadense, Nicotiana tabacum, Oryza sativa, Phaseolus vulgaris, Pisum sativum, Spinacia oleracea, Vanilla planifolia, Zea mays*). The comparison revealed both conserved and divergent patterns in gene arrangement (Supplementary Table 2). The *psbN/psbH* (BDP3) pair maintained a bidirectional organization across all examined species, indicating strong structural conservation. The *atpA/rbcL* pair (BDP1) was bidirectional in *E. elegans*, *P. tricornutum*, and *V. carteri* while in *K. corcontica, I. terricola*, and in all higher plants, *rbcL* in BDP1 was conserved but *atpA* was replaced by *atpB*, suggesting functional substitution or evolutionary rearrangement. The *chlL/petB* pair (BDP2) preserved a bidirectional arrangement exclusively in *E. elegans*, *G. pectorale*, and *V. carteri*, but was absent or rearranged in others, highlighting lineage-specific conservation. The *rpoB-1/psbF* pair (BDP4) was not conserved in any species; although *psbF* persisted in higher plants, it was repositioned, often losing its bidirectional relationship with *rpoB-1*. These analyses indicate that BDP1–3 represent conserved bidirectional promoters, with strict conservation of BDP3, whereas BDP4 is non-conserved. Based on their defined promoter signatures, BDP1, BDP2, and BDP3 were selected for further functional characterization as candidate BDPs.

Generation of *C. reinhardtii* transplastomic cell lines with mono- and bidirectional expression cassettes

Following chloroplast DNA isolation, the three putative BDP IRs with their corresponding 5' UTR were amplified (Supplementary Figs. 2 and 3, Supplementary Table 3 and Supplementary Data 1) and cloned to generate chloroplast expression vectors (pABDP1, pABDP2, and pABDP3; Fig. 2, and Supplementary Table 4). Each vector incorporated the candidate IR between the codon-optimized sequences of the fluorescent proteins mVenus and tdTomato. The monodirectional *psbD/* 5′ UTR[24] promoter was amplified as well, cloned, and used to drive *mVenus* and *tdTomato* expression as positive controls on separate vectors, pAMVe and pATDt, respectively (Fig. 2). *mVenus* was flanked by the *psbA* /3′ UTR, while *tdTomato* was flanked by the *rbcL/* 3′ UTR in both mono- and bidirectional constructs, as these terminators exhibit consistent and reliable performance in transgene expression in *C. reinhardtii* chloroplast[11,48–51]. Constructs were designed for integration into the chloroplast genome of the mutant strain CC4388 via homologous recombination at the *psbN-trnE2* locus, a well-established site for chloroplast transformation in *C. reinhardtii*[52]. This strain is photosynthetically deficient, as the essential *psbH* gene has been replaced by the *aadA* marker gene, conferring resistance to spectinomycin/streptomycin. Homologous recombination restores the *psbH* gene, enabling the selection of transplastomic lines based on the recovery of photosynthetic activity on high-salt minimal (HSM) medium. Recombinant vectors were validated by restriction enzyme digestion and complete plasmid sequencing (Supplementary Data 2). These vectors (pABDP1, pABDP2, pABDP3, pAMVe, and pATDt) were subsequently introduced into the chloroplast genome by particle bombardment, yielding transplastomic cell lines designated P1, P2, P3, mV, and tdT, respectively (Supplementary Fig. 4a).

Cassette integration and homoplasmy were verified by PCR screening using a three-primers strategy (Supplementary Fig. 4b). Although faint, distinct amplicons of 2.8, 2.7, and 1.8 kb were detected in transplastomic lines P1, P2, and tdT, respectively. In contrast, the parental CC4388 strain exhibited a 1.0 kb band (Supplementary Fig. 4c and Supplementary Fig. 5a–c). These results confirm the transgene cassettes' site-specific integration and the homoplasmy establishment. Homoplasmy could not be confirmed in P3 transplastomic cell lines, while mV transplastomic lines exhibited a heteroplasmic genotype (Supplementary Fig. 4c and Supplementary Fig. 5b), indicating the coexistence of transformed and untransformed chloroplast genome populations[53]. To resolve this, P3 and mV transplastomic cell lines underwent three additional rounds of restreaking on HSM-agar under selective pressure to promote photosynthetic restoration. Homoplasmy was subsequently validated by the loss of spectinomycin resistance in TAP-agar supplemented with 100 μg/mL spectinomycin.

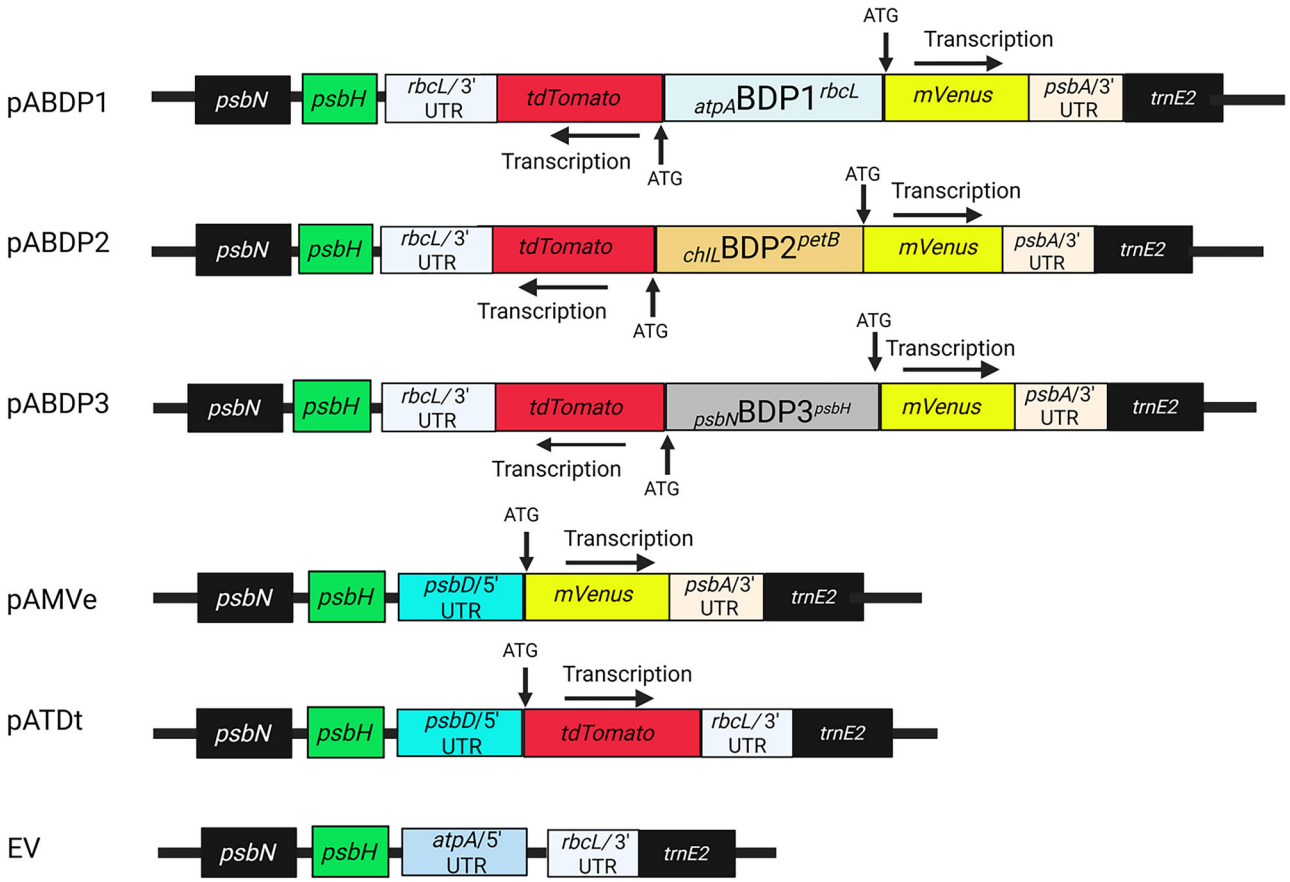

Fig. 2 | Genetic design of bidirectional and monodirectional constructs for transgene expression in the C. reinhardtii chloroplast. Constructs were engineered to enable the simultaneous expression of two fluorescent reporters, *mVenus* and *tdTomato*, in opposite orientations under the control of endogenous bidirectional promoters (BDP1–BDP3) or in a monodirectional configuration. Bidirectional constructs (top three maps) feature native intergenic regions identified as BDP1 (*atpA/rbcL*), BDP2 (*chlL/petB*), and BDP3 (*psbH/psbN*), each driving divergent expression of *mVenus* and *tdTomato*. Fluorescent genes are flanked by 3′ UTRs from *psbA* (mVenus) and *rbcL* (tdTomato). Monodirectional constructs (bottom two maps) express either *mVenus* or *tdTomato* individually, using the *psbD* 5′ UTR as the promoter and the *psbA* or *rbcL* 3′ UTR as terminators. The chloroplast expression vector pASapI was used as empty vector (EV)[52]. Homologous recombination sites (*psbN* and *trnE2*) located at each end of the constructs ensure site-specific integration into the chloroplast genome. Arrows indicate the orientation of transcription. These configurations were used to assess the ability of native bidirectional promoters to mediate coordinated and balanced expression of multiple transgenes in the plastome of *C. reinhardtii*.

Bidirectional co-expression of fluorescent proteins in *C. reinhardtii* chloroplasts

Heterologous expression of *mVenus* and *tdTomato* was quantified by RT-qPCR at day 5 of growth to assess candidate promoters activity in *C. reinhardtii* chloroplast transformants (Fig. 3)[54]. *tdTomato* was robustly expressed in all three transplastomic lines of tdT, P1, and P2, while very low expression was detected in only one of three P3 transformants. In contrast, the monodirectional *psbD*/5′ UTR (MDP) produced more uniform expression. Expression levels of *tdTomato* were higher in tdT controls, P1, and P2 compared to P3 positive transformants (Fig. 3a–d). *mVenus* was expressed in all mV, P1, P2, and P3 transplastomic lines, with P1, P2, and mV exhibiting higher expression levels than P3. BDP3 displayed a striking 10,000-fold and 1000-fold reduction in expression levels of *tdTomato* and *mVenus*, respectively, relative to the *psbD*/5′ UTR, BDP1, and BDP2 promoters. P1 lines expressed ~3-fold more *mVenus*, but similar level of *tdTomato* compared to the respective MDP controls. These results show that BDP1 and BDP2 can drive bidirectional transcription in the *C. reinhardtii* chloroplast, with BDP1 and BDP2 displaying a more balanced expression in both directions and BDP3 exhibiting low levels and pronounced directional asymmetry. Conceptual models of transcription initiation from the bidirectional and monodirectional architectures are provided (Fig. 3e, f). These schematics illustrate how mirrored promoter elements within BDPs enable recruitment of the chloroplast RNA polymerase complex in both orientations, whereas the *psbD*/5′ UTR promoter directs transcription unidirectionally toward a single reporter gene.

Bidirectional protein synthesis from BDP1 in *C. reinhardtii* chloroplasts

Following confirmation of chimeric mRNA expression in the chloroplast of *C. reinhardtii*, we tracked cell growth and the fluorescence of chlorophyll, mVenus, and tdTomato (Fig. 4a, b and Supplementary Figs. 6, 7, and 8) in three independent transplastomic cell lines per construct over 13 days. Fluorescence analysis revealed increased accumulation of mVenus and tdTomato in mV, tdT, and P1 transformants throughout the culture period (Fig. 4a, b). To characterize further expression dynamics, all clones growing under selective conditions were analyzed via flow cytometry in both exponential (Exp) and stationary (Sta) phases (Fig. 4c–e and Supplementary Data 3). In the exponential phase, fluorescent cells were detected in 28/30 (93.3%), 7/7 (100%), 7/7 (100%), 0/4 (0%), and 3/7 (42.9%) transplastomic cell lines from mV, tdT, P1, P2, and P3 transformants, respectively. In the stationary phase, fluorescent cells were observed in 31/33 (93.9%), 15/15 (100.0%), 13/13 (100.0%), 3/6 (50.0%), and 4/10 (40.0%) transplastomic cell lines, respectively (Supplementary Fig. 9). Western blot analysis confirmed the detection of a 27 kDa mVenus band in mV ($n = 3/3$), P1 ($n = 3/3$), P2 ($n = 3/3$), and P3 ($n = 1/3$) transformants on day 13 (Supplementary Fig. 10), although the band was faint in the case of P2 and P3. The mean

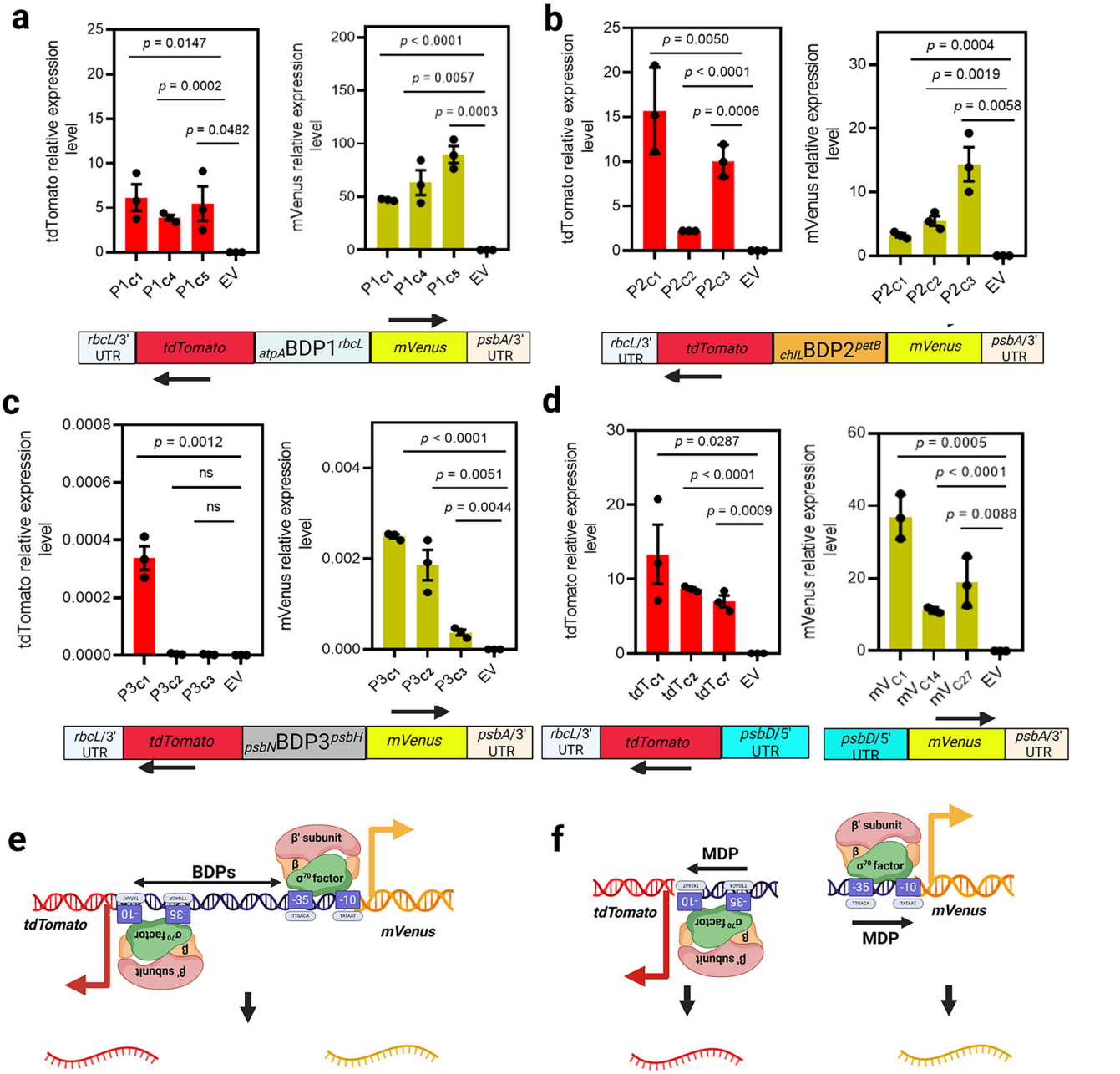

Fig. 3 | Bidirectional promoter regions mediate divergent transcription of heterologous genes in the C. reinhardtii chloroplast. Expression analysis of transplastomic lines carrying bidirectional (BDP1–BDP3) and monodirectional (*psbD* 5′ UTR) promoter constructs. **a–c** Reporter gene expression levels of *mVenus* and *tdTomato* in three independent lines for each bidirectional construct (P1–P3). **d** Reporter gene expression levels in monodirectional constructs expressing either *mVenus* or *tdTomato*. **e**,**f** bidirectional and monodirectional transcriptional model of (PEP)-dependent promoters in *C. reinhardtii* chloroplast. Expression was quantified by RT-qPCR using three biological replicates per clone. Gene expression values were normalized to endogenous reference genes (*GBLP* and *histone 3*) and reported as relative expression levels (mean ± s.d.). Construct schematics below each graph depict the genetic configuration and orientation of the reporter genes, including their corresponding untranslated regions (UTRs) and promoter sequences. Arrows represent the transcriptional direction. Data were analyzed by unpaired two-tailed *t*-tests to assess differences between transplastomic lines and empty vector (EV) controls. *p*-values are indicated above the bars, ns, not significant.

frequency of fluorescent cells was 21.3% for mV and 72.8% for tdT transformants, with corresponding mean fluorescence intensities (MFIs) of 2298.1 and 18,441.6, respectively. The mean frequency of tdTomato$^+$mVenus$^+$ fluorescent cells in P1, P2, and P3 transformants was 82.8%, 26.7%, and 5.2%, with respective tdTomato MFIs of 52,799.7, 730.3, and 956.3; and mVenus MFIs of 1757.9, 1030.3, and 1092.7. Notably, tdTomato signal from BDP2-driven expression increased drastically in three lines during stationary growth (MFI = 2,414.3). Despite a three-fold increase in *mVenus*, P1 lines displayed slightly lower MFI compared to mV lines. Conversely, they accumulated ~3-fold more fluorescent proteins per cell compared to tdT lines. These findings underscore the expression and accumulation of fluorescent proteins in *C. reinhardtii* chloroplasts, with BDP1 exhibiting the strongest bidirectional activity at both mRNA and protein levels. The results also suggest differential post-transcriptional regulatory mechanisms between the BDPs.

Efficient targeting and retention of transgenic proteins driven by BDP1 within the chloroplast

Next, we examined the subcellular localization of the fluorescent reporters to assess their intracellular fate. As plastid-targeted transgenes are generally

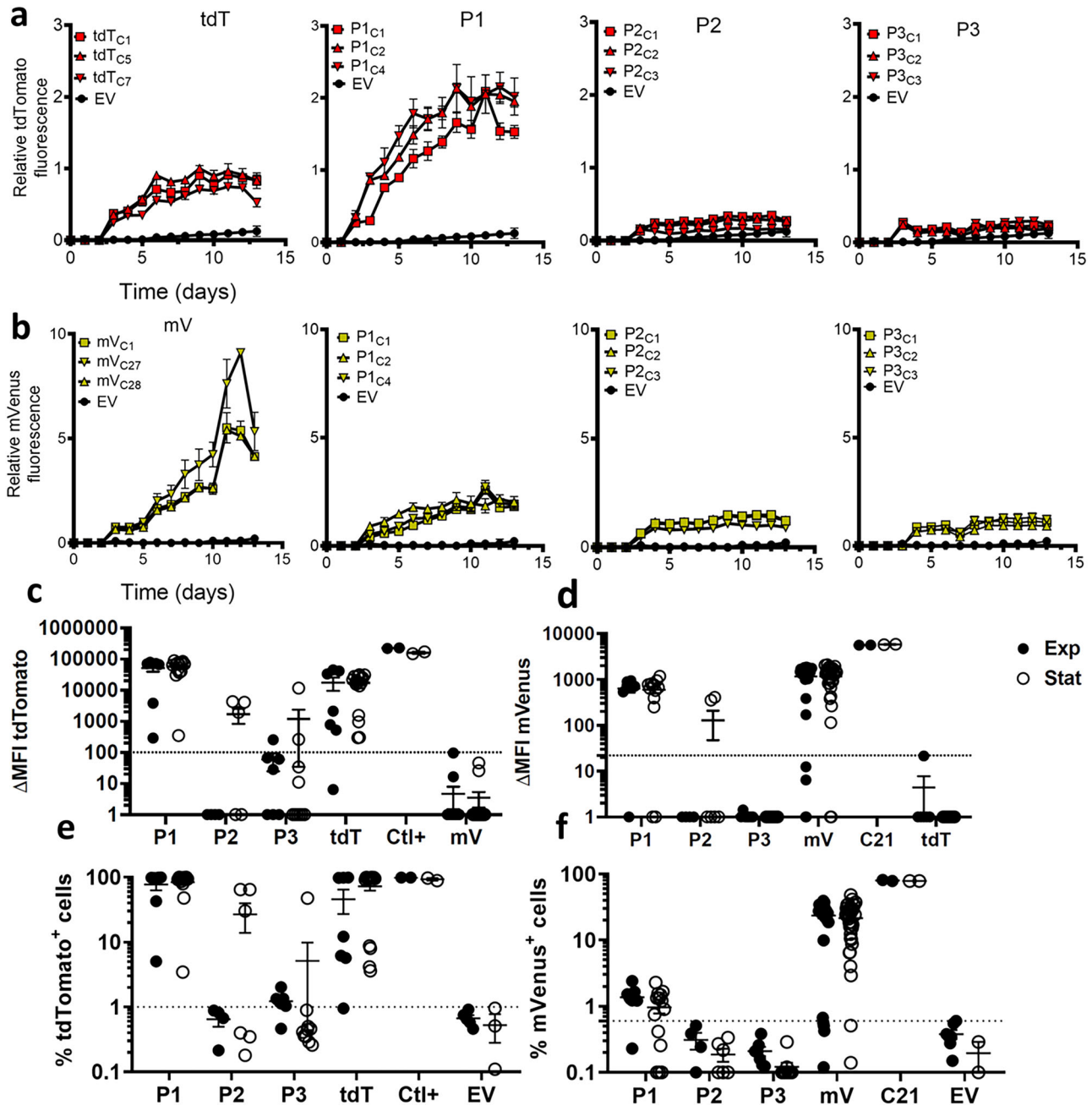

Fig. 4 | Functional analysis of bidirectional promoter activity in the chloroplast of *C. reinhardtii*. **a**,**b** Time-course analysis of mVenus and tdTomato fluorescence in strains carrying bidirectional promoter constructs (P1–P3) compared to mono-directional control strains expressing either mVenus (mV) or tdTomato (tdT) under the *psbD* 5′ UTR promoter. Fluorescence signals were measured over 13 days and normalized to chlorophyll (Chl) content using a Synergy H4 microplate reader and Gen5 2.07 software. **c** Flow cytometry analysis of tdTomato mean fluorescence intensity (MFI) in transformant clones during exponential (Exp) and stationary (Stat) phases. **d** Flow cytometry analysis of mVenus fluorescence intensity in transformant clones during exponential (Exp) and stationary (Sta) growth phases. Mean fluorescence intensity (MFI) values represent the difference in signal between each sample and the mean fluorescence intensity of the empty vector (EV) control. Values below EV background were set to 1 for graphical clarity. **e** Percentage of tdTomato$^+$ cells in each transformant clones during exponential (Exp) and stationary (Sta) growth phases. **f** Percentage of mVenus$^+$ cells in each transformant clones during exponential (Exp) and stationary (Sta) growth phases. Fluorescence percentages above background levels observed in the EV control were considered positive. Background thresholds were set at 1% for tdTomato and 0.6% for mVenus. Values below these thresholds were fixed at 0.1% to facilitate representation. A total of 30, 7, 7, 4, and 7 clones were analyzed for mV, tdT, P1, P2, and P3 strains, respectively, in the exponential phase; and 33, 15, 13, 6, and 10 clones, respectively, in the stationary phase. Cells were gated based on forward scatter area (FSC-A) and side scatter area (SSC-A) parameters. Chlorophyll autofluorescence was detected in the PerCP channel (690/50 nm), excluding non-specific autofluorescence in the PB450 channel (450/45 nm). mVenus fluorescence was analyzed in the FITC channel (524/40 nm), while tdTomato fluorescence was detected in the PE channel (585/42 nm BP) (see Supplementary Fig. 9 for gating strategy). A clone expressing the *mVenus* reporter gene in the nucleus under the HSP70-rbcS2 promoter (C21) was used as a positive control for *mVenus*. The CC4388 strain treated with 10% DMSO and propidium iodide (PI) was used as a positive control for *tdTomato* (Ctl +), which emit fluorescence overlapping with the tdTomato channel. Error bars represent standard deviation (sd) from three biological replicates.

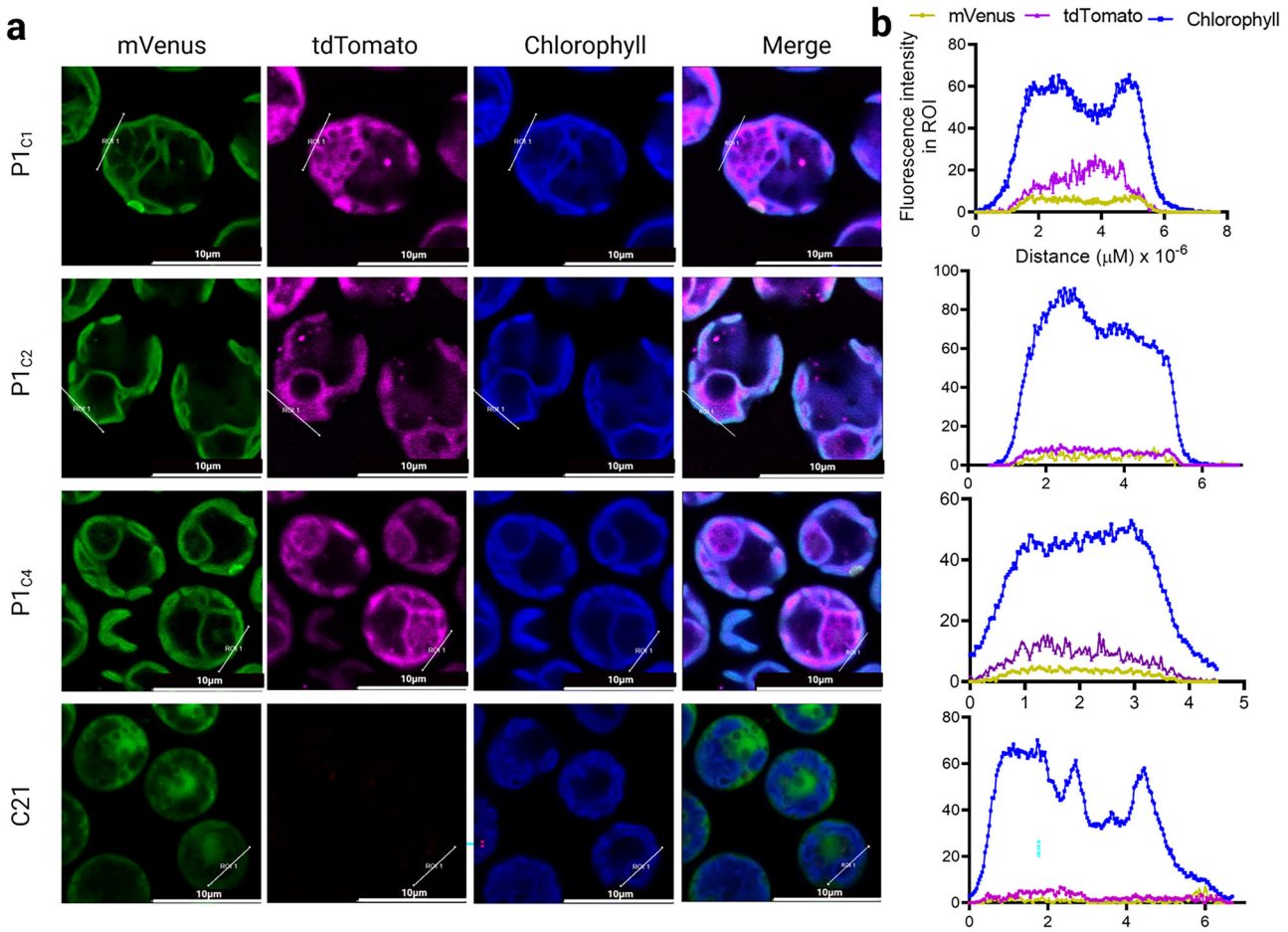

Fig. 5 | Subcellular localization of mVenus and tdTomato fluorescent proteins in *C. reinhardtii* chloroplast transplastomic lines. Confocal microscopy and fluorescence intensity profile analyses of transplastomic lines expressing mVenus (yellow) and tdTomato (magenta). **a** Representative fluorescence micrograph of individual clones (P1C1, P1C2, P1C4, and C21), with separate channels for chlorophyll autofluorescence, mVenus, and tdTomato, as well as merged images. **b** Fluorescence intensity profiles across regions of interest (ROIs), highlighting the spatial distribution and relative signal intensities of mVenus, tdTomato, and chlorophyll within the cell. ROI 1 delineates the chloroplast and cytosolic compartments, enabling distinction of protein localization. All images were acquired five days post-inoculation using confocal laser scanning microscopy. Scale bar, 10 µm.

retained within the organelle[2], we employed confocal microscopy to analyze three independent P1 transplastomic lines (Fig. 5a, b). We used C21, which expresses the *mVenus* reporter gene in the nucleus under the *HSP70-rbcs2* promoter, as a control strain of cytoplasmic localization. Fluorescence intensity profiling across the chloroplast (region of interest 1, ROI 1) revealed a strong colocalization of mVenus and tdTomato with chlorophyll autofluorescence (Fig. 5b), confirming efficient retention of both proteins within the plastid. These findings validate the proper localization of the reporters and reinforce the potential of the *C. reinhardtii* chloroplasts as a robust compartment for recombinant protein production and accumulation.

Exogenous methyl jasmonate selectively boosts BDP1 promoter-driven expression in *C. reinhardtii* chloroplasts

Previous studies have shown that MeJA modulates gene expression in various organisms, including the microalga *C. reinhardtii*. Notably, Commault, et al.[33] demonstrated that treating cells in the mid-exponential growth phase with 1 mM MeJA up-regulated key nuclear genes encoding enzymes of the chloroplast-localized MEP pathway. More recently, heterologous expression of a MYB transcription factor from *Salvia miltiorrhiza* has been shown to activate gene expression in *C. reinhardtii*, highlighting the potential of MYB-mediated regulatory circuits in microalgal systems[55]. MeJA is thought to exert its regulatory effects in part through the activation of specific transcription factors, such as MYB and MYC[56,57], which can influence the expression of nuclear and possibly plastidial genes (Fig. 6a). To further characterize BDP1 and enhance the production of recombinant proteins, we tested the effect of MeJA treatment on transgene expression. Specifically, 0.5 mM MeJA was applied during the mid-exponential growth phase to stimulate transgene expression and protein accumulation earlier in the culture cycle, potentially reducing the time required to achieve higher yields. As a reference for the in-silico analysis of MeJA-responsive elements in BDP1, we included four putative nuclear promoters, i.e., geranyl diphosphate synthase (GPPS), solanesyl diphosphate synthase (SPPS), farnesyl diphosphate synthase (FPPS), and geranylgeranyl diphosphate synthase (GGPPS) (Supplementary Table 3), which drive expression of nucleus-encoded, chloroplast-targeted enzymes involved in isoprenoid biosynthesis. These promoter regions were subjected to in-silico analysis to identify predicted MYB and MYC transcription factor binding sites (Fig. 6b). Treatment with MeJA led to an increase in tdTomato fluorescence intensity across all three independent P1 transplastomic cell lines (P1C1, P1C2, and P1C4), with significant differences observed between MeJA-treated and untreated cells (P1C1, $p < 0.001$; P1C2, $p < 0.01$; P1C4, $p < 0.05$), while only P1C1 displayed a significant increase in mVenus fluorescence intensity ($p < 0.05$). A change of 1.5-fold (from 1.0 to 2.5 at day 5), 0.5-fold (from 0.8 to 1.3 at day 7), and 1.2-fold (from 0.9 to 2.1 at day 7) in tdTomato fluorescence was observed compared to untreated cells (Fig. 6c–e). Further supporting these findings, an analysis of the relative transcript levels of *tdTomato* in the P1C1 transplastomic cell line 24 h after

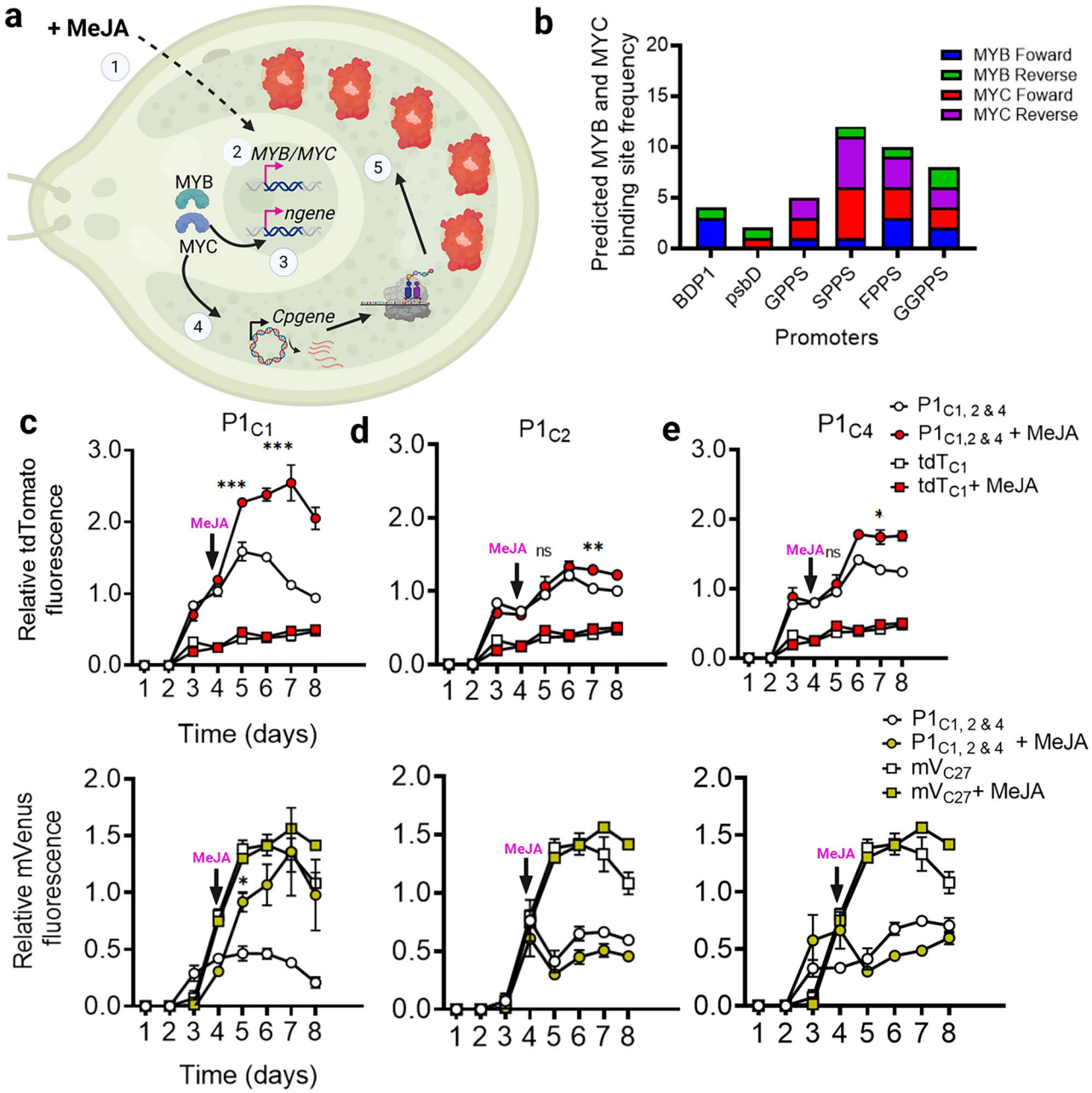

Fig. 6 | Methyl jasmonate enhances tdTomato expression in chloroplast transplastomic lines. a Schematic overview of the proposed mechanism of MeJA action. Upon MeJA treatment (1), MYB and MYC transcription factors (2), known to be MeJA-inducible, are activated in the nucleus and may translocate or signal toward the chloroplast (3), where they potentially regulate transgene expression via binding to native promoter elements (4), enhancing transcription of the transgene of interest (5). ngene: nuclear gene; Cpgene: chloroplast gene. **b** In silico prediction of MYB and MYC transcription factor binding sites in the promoter of BDP1, *psbD*, and the nuclear genes *GPPS*, *SPPS*, *FPPS*, and *GGPPS*. Binding site frequencies for MYB (forward/reverse strands) and MYC (forward/reverse strands) were determined using PLACE database tools. **c–e** Time-course quantification of tdTomato and mVenus fluorescence in three independent P1 transplastomic lines (P1C1, P1C2, and P1C4) over 8 days following MeJA treatment. Error bars represent standard deviation (sd) from three biological replicates. Asterisks indicate statistical significance compared to control at each time point (unpaired t-test, $^{*}p < 0.05$; $^{**}p < 0.01$; $^{***}p < 0.001$; ns: not significant).

MeJA treatment revealed a significant increase compared to untreated cells (Supplementary Fig. 11). This suggests that the tdTomato fluorescence increase was correlated with transcript levels. These findings demonstrate that exogenous MeJA can selectively enhance BDP1 promoter-driven transgene expression in the chloroplast of *C. reinhardtii*, particularly boosting tdTomato expression at both transcript and protein levels.

Discussion

Microalgal chloroplasts are increasingly targeted for engineering high-value metabolic pathways[49,58,59]. However, harnessing their full potential, particularly for introducing complex metabolic pathways, requires more advanced regulatory elements for precise control of multigene expression. In this study, we identified and functionally characterized native bidirectional promoters from the chloroplast genome of *C. reinhardtii*, and for the first time, demonstrated h2h transgene expression in this system.

By scanning the complete chloroplast genome of *C. reinhardtii*, we identified four gene pairs, *atpA/rbcL*, *chIL/petB*, *psbH/psbN*, and *rpoB-1/psbF*, organized in a h2h configuration separated by IRs of 855 bp, 632 bp, 570 bp, and 1056 bp, respectively. *atpA/rbcL* IR includes the well-established promoter *rbcL* and its 5' UTR, commonly used as MDP in *C.*

reinhardtii genetic engineering to regulate expression[26,51]. Promoter motif analysis revealed putative -10 and -35 elements within IRs of *atpA/rbcL*, *chlL/petB*, and *psbH/psbN*, albeit at non-canonical distances in the latter two cases. This analysis reinforced that the identified IRs may act as BDP. This spatial separation, along with their prokaryote-like architecture, is consistent with the notion that chloroplast transcription may involve DNA looping or higher-order structural mechanisms for promoter activity modulation[60]. This suggests that, beyond sequence conservation, the three-dimensional architecture of these IRs may play a pivotal role in modulating bidirectional promoter activity. Conservation analysis across fifteen additional species of microalgae and higher plants revealed that *psbH/psbN* IR is highly conserved, an ancient and functionally constrained co-evolution of the adjacent *psbH* and *psbN* genes, both of which encode phosphoprotein subunits of photosystem II, integral to the photosynthetic machinery[61,62]. These proteins' shared function and organelle localization may underlie their evolutionary linkage. In contrast, the *chlL/petB* IR displayed a bidirectional organization exclusively within Volvocine algae (*Volvocaceae* + *Chlamydomonaceae*) lineages (*E. elegans, G. pectorale*, and *V. carteri*), suggesting that this architecture constitutes a derived feature that emerged relatively recently during the diversification of these lineages. Conversely, the *rbcL* intergenic region showed bidirectionality in three microalgal species and was conserved in all higher plants, consistent with an ancestral BDP retained across major photosynthetic lineages. Notably, a bidirectional arrangement of the *atpA/rbcL* pair was present in *E. elegans*, *P. tricornutum*, and *V. carteri*, whereas in *K. corcontica*, *I. terricola*, and all higher plants, *atpA* is replaced by *atpB*, indicating possible genome rearrangements or functional substitutions during chloroplast evolution. By contrast, the *rpoB-1/psbF* pair showed no conservation across any lineage, implying a lineage-specific loss or extensive genomic reorganization. Collectively, these observations support the hypothesis that some BDPs regions represent ancestral genomic features retained in select taxa, while others, such as *chlL/petB* among volvocines, have likely emerged independently through recent evolutionary innovation. Based on promoter signature analysis, three candidate regions, BDP1, BDP2, and BDP3 were selected for functional characterization.

IRs of *atpA/rbcL* (BDP1), *chlL/petB* (BDP2), and *psbN/psbH* (BDP3) were then functionally characterized by testing their ability to co-express two heterologous fluorescent reporter genes (*mVenus* and *tdTomato*) in opposite orientations in the chloroplast of the alga. RT-qPCR analysis revealed that all three IRs exhibited transcriptional activity from both directions, although BDP3-driven transcription was very low. To our knowledge, this is the first report of functional characterization and bidirectional transcription of a heterologous gene from native chloroplast IRs in *C. reinhardtii*. Among the three regions tested, BDP1 and BDP2 achieved relatively balanced expression of both transgenes in both directions compared to MDPs[63,64]. However, expression levels varied among independent P2 transformants, despite detected homoplasmy and identical expression cassettes integrated at the same locus. Such variability, often attributed to the "transformosome" effect, may result from stochastic transformation-associated events, plastome copy number variation, or clone-specific physiological states[63,64]. Such variation underscores the importance of analyzing multiple independent lines to draw accurate conclusions about promoter activity and regulatory effects. In contrast, BDP1 lines showed higher and more consistent expression of *mVenus* and moderate expression of *tdTomato*, compared to controls. Previous studies indicated that the corresponding downstream IR of BDP1, which contains the promoter/5' UTR regulatory regions of the *rbcL* gene, resulted in a 9-fold decrease in chimeric mRNA levels of heterologous *gfp* in the chloroplast of *C. reinhardtii*, compared to the *psbD*/5' UTR promoter[65]. In contrast, our study shows that using the entire *atpA/rbcL* IR as a BDP significantly enhances the transcripts levels, achieving *mVenus* expression levels comparable to those obtained with the *psbD*/5' UTR promoter. Interestingly, despite driving expression of its endogenous targets (*psbN*, *psbH*)[18], the BDP3 IR failed to support robust heterologous bidirectional transcription in our system. In chloroplasts, 5′ and 3′ ends are key determinants of mRNA stability/maturation and translation[66]. The *rbcL* and *psbA* 3′ UTRs used in our constructs contain inverted repeats that form protective stem-loop structures, which ensure basal transcript stability by preventing 3′ → 5′ exonucleolytic degradation[67,68]. Therefore, in addition to the promoter core, the major determinants of transcript stabilization, maturation, and translation in our chimeric constructs are likely shifted toward the 5′ UTRs of the adjacent gene pairs present in each BDP. A plausible explanation for the weak BDP3-driven expression of *mVenus* and the almost complete absence of *tdTomato* expression includes degradation of the transcripts by chloroplast 5′ → 3′ exonucleases, which preferentially target mRNAs that lack strong footprints of RNA stability/maturation factors[69]. It is conceivable that the nucleus-encoded MBB1 factor, which specifically binds to the 5′ UTR of the endogenous *psbH* transcript, provided partial stabilization of the chimeric *mVenus* transcript, thereby allowing the detection of low transcript accumulation. In contrast, the chimeric *tdTomato* transcript harboring the *psbN* 5′ UTR likely remained more vulnerable to degradation by 5′ → 3′ exonucleases. In addition, it is possible that BDP3 harbors specific sequence features that are co-adapted to its native *psbN* and *psbH* gene contexts, possibly through interactions with sequence elements or binding sites embedded within the endogenous coding regions[70]. Such co-evolved regulatory elements could reinforce BDP3-driven transcription and the accumulation of stable, mature mRNAs in its natural genomic setting. In contrast, their absence in heterologous reporter constructs likely contributes to reduced transcriptional efficiency[65].

At the protein level, BDP1 was the only region to drive sustained accumulation of both fluorescent proteins over a 13-day culture period under mixotrophic conditions. Both mVenus and tdTomato accumulated and remained in the microalgae chloroplast. However, although BDP1-driven *mVenus* expression produced high transcript levels, protein accumulation, as measured by flow cytometry was moderate. Conversely, tdTomato accumulated to similar or even higher levels despite similar transcript abundance. Although the flow cytometer is more optimized to excite tdTomato (91% excitation at 561 nm) than mVenus (35% excitation at 488 nm), this result is also consistent with the extensive literature describing post-transcriptional control of chloroplast gene expression in *C. reinhardtii* mediated by NTAFs M or T factors. For instance, the 5′ UTR of *atpA* transcript requires the nuclear-encoded MDA1 and TDA1 factors for mRNA stability and efficient translation initiation[71–74], while *rbcL* mRNA stability depends on MRL1 and PPR1[31,75]. These examples highlight how nuclear-encoded factors influence transcript stability and translation efficiency. This suggests that the chimeric *tdTomato* transcripts may be translated more efficiently than the chimeric *mVenus* transcripts, resulting in higher protein accumulation despite lower transcript levels. In contrast to BDP1, transplastomic lines harboring BDP2 exhibited much lower fluorescence intensity and protein accumulation, despite comparable accumulation of the chimeric transcript compared to MDP controls. Interestingly, tdTomato signals from BDP2-driven expression increased during stationary growth, suggesting that BDP2 activity is coupled to the cellular metabolic state. This shift likely reflects cells transition from rapid growth to nutrient limitation, where specific RNA-binding proteins or translational activators may differentially affect the *chlL*-derived 5′ UTR of BDP2[76]. Consistently, previous studies have also reported low recombinant protein yields when using the *chlL* 5′ UTR (derived from the upstream region of BDP2)[66]. The nuclear factor PPR1 (TCB1) is required for stabilization/translation of the *petB* mRNA. However, little information is available regarding the M and T factors specific to the *chlL* gene, although footprints of M factors have been detected upstream of its transcription initiation site. In this scenario, the chimeric *mVenus* and *tdTomato* transcripts produced by BDP2 should not only be accumulated but also translated into their corresponding proteins. Thus, the discrepancy observed between transcript and protein levels in P2 transformants could be explained by a relative deficit of M and T factors, caused by an excess of chimeric and endogenous transcripts that share the *petB* and *chlL* 5′ UTRs. These observations were made under mixotrophic conditions in TAP medium, where chloroplast transcript levels correlated well with those of HSM. However, variations in

the availability of NTAFs suggest that future studies should assess BDP-driven expression under phototrophic conditions. Such analyses would be particularly relevant for industrial applications and may reveal distinct regulatory inputs affecting BDP performance during photoautotrophic growth. More broadly, these results highlight that, for optimal recombinant protein production in the chloroplast, the balance between available M/T factors and competing transcripts is a key determinant. The choice of 5′ UTR directly influences this competition, as each UTR recruits a specific set of nucleus-encoded factors. An overload of chimeric transcripts using the same regulatory elements as highly expressed endogenous mRNAs may lead to dilution or competition for M/T factors, thereby limiting the translational efficiency of recombinant transcripts. Conversely, the use of 5′ UTRs that mobilize factors less engaged by native genes could improve translation and accumulation of heterologous proteins. To potentially address these limitations, targeted modifications of the 5′ UTRs in both the forward and reverse orientations of the bidirectional promoter's IRs could be explored. Specifically, replacing the native 5′ UTRs of BDP2-3 with the mature 5′ UTR of *psbD*, *psaD*, or *rps4* mRNAs has been shown to markedly enhance recombinant protein accumulation, as demonstrated in our monodirectional reporter constructs for *psbD*/5′ UTR and previous chloroplast engineering studies[77–79]. The *rps4* 5' UTR, in particular, is recognized for its robust interaction with mRNA-binding factors, enhancing transcript stability and translation efficiency in a promoter-dependent manner[67]. Such a strategy could boost the bidirectional expression potential of BDP2, which already ensures balanced transcription of both transgenes but with limited protein yield.

Finally, the ability of MeJA to enhance BDP1 activity during the exponential growth phase was assessed. In higher plants, MeJA is known to induce gene expression through a complex signaling pathway involving key components, such as the jasmonate receptor coronatine insensitive 1 (COI1)[80–82] and jasmonate ZIM-domain (JAZ) proteins[83,84]. Under normal conditions, JAZ proteins repress transcription by binding to transcription factors, such as MYC2[56,85]. Upon stress perception, MeJA levels increase, allowing MeJA to bind the COI1 receptor as part of an SCF-COI1 complex, which targets JAZ proteins for ubiquitination and subsequent degradation via the 26S proteasome[56,57]. This degradation releases MYC2 and other transcription factors, enabling them to activate transcription by binding to MeJA-responsive elements in target gene promoters. While MeJA is primarily known for regulating nuclear gene expression, recent studies suggest that retrograde and anterograde signaling pathways can impact chloroplast gene expression as well. For instance, MeJA treatment has been shown to modulate photosynthetic activity, plastid development, and retrograde signaling pathways that coordinate nuclear and plastid gene expression. In *C. reinhardtii*, Commault, et al.[33] reported MeJA-induced upregulation of key MEP pathway enzymes that translocate to the chloroplast. MEP enzymes are nucleus-encoded and post-translationally imported into the chloroplast for terpenoid biosynthesis. Although the MeJA signaling pathway remains poorly characterized in microalgae, it may influence chloroplast gene expression either indirectly through nuclear factors, such as MYC and MYB, which bind to promoter sequences and modulate transcription, or through M- and T-factors that stabilize chloroplast transcripts and promote their translation. Recent studies have demonstrated the potential of *MYB* to activate gene expression in the microalgae *C. reinhardtii*, including the induction of a heterologously expressed *MYB* transcription factor from *Salvia miltiorrhiza*[55]. In silico analysis confirms the presence of *MYB* and *MYC* binding sites in four putative promoter sequences of *GPPS, SPPS, FPPS*, and *GGPPS* genes, as well as BDP1. In our study, MeJA treatment significantly increased tdTomato fluorescence in all three independent P1 transplastomic cell lines, which may reflect such cross-compartment regulatory effects. In contrast, mVenus fluorescence remained unaffected in two out of three clones, suggesting directional responsiveness of BDP1 to MeJA. Given that MeJA is closely linked to defense responses and specialized metabolism[56,83–85], the chloroplast likely upregulates genes involved in these pathways, suggesting a possible implication of RbcL and AtpA in these processes. While the molecular basis of this regulation remains to be elucidated, our results provide a foundation for further exploration of jasmonate signaling as a tool to fine-tune recombinant protein production from the chloroplast.

In summary, this study combines evolutionary and functional analyses to provide a comprehensive characterization of three IRs in the *C. reinhardtii* chloroplast genome that exhibit intrinsic BDP activity. Conservation analysis across microalgae and higher plants revealed highly variable evolutionary trajectories of chloroplast IRs. The *psbH*/*psbN* IR is deeply conserved across Archaeplastida, consistent with an ancestral BDP organization maintained throughout plastid evolution. In contrast, the *chlL*/*petB* IR displayed a bidirectional configuration exclusively within Volvocine algae, indicating that this architecture represents a derived feature that emerged relatively recently during Volvocine diversification. Conversely, the *atpA*/*rbcL* IR exhibited bidirectionality in multiple microalgal species, and all higher plants instead harbor an atpB/rbcL configuration, suggesting chloroplast genome rearrangements or functional substitutions during evolution, as well as the complete loss of *rpoB-1*/*psbF*. Functionally, we showed that BDP1 supported expression of two fluorescent reporters in opposing orientations, highlighting its potential as a compact alternative to MDPs for synthetic biology applications. By contrast, BDP2 and BDP3 were more strongly influenced at the post-transcriptional level, suggesting a key role for mRNA maturation/translation factors and transcript competition in determining protein accumulation. Interestingly, exogenous application of MeJA selectively enhanced tdTomato expression driven by BDP1, suggesting a potential strategy for chemically inducible transgene expression in chloroplasts.

Future work should explore the versatility of BDP1 in diverse genetic contexts and chassis, including bicistronic operons for expression of multiple proteins. Refinement of BDP function could also be achieved through targeted 5′ UTR modifications, testing the efficiency of control promoters, such as the *psbD*/ 5′ UTR in head-to-head configurations, comparative screening of BDP1 IR from higher plants and microalgae in *C. reinhardtii*, and alternative design permutations (pairing mVenus with *rbcL*/3′ UTR). These strategies may expand the interest of BDPs and enhance the potential of algal platforms not only for sustainable production of biofuels, pharmaceuticals, and other valuable compounds, but also as versatile systems to investigate gene regulation mechanisms and synthetic biology design principles.

Methods

Microbial strains and growth conditions

The *Escherichia coli* strains NEB® 10-beta (New England Biolabs, Canada), used for plasmid extraction, was cultured in Luria–Broth medium (LB) supplemented with ampicillin (100 mg/L; Lot 197674, Fisher Scientific, China). The microalga mutant strain CC-4388 (*psbH*: *aadA*, mt + ; Chlamydomonas Resource Center; http://www.chlamycollection.org) was used for chloroplast transformation. This strain, deficient in photosynthesis, has the vital photosynthetic gene *psbH* replaced by the *aadA* gene, conferring resistance to spectinomycin/streptomycin[52]. Homologous recombination enabled the restoration of the *psbH* photosynthetic gene, allowing the selection of transplastomic lines based on restored photosynthetic activity on HSM rather than antibiotic resistance. Cell lines were initially selected on selective agar plates Tris-acetate phosphate (TAP) with spectinomycin (Lot Q6100160, BIO BASIC, Canada) at 100 µg/mL for *aadA* selection and maintained on TAP agar plates under dim light conditions (5–10 µmol $m^{-2}s^{-1}$) at a temperature of 20 °C.

Selection of putative bidirectional promoters and structures analysis

The arrangement of each gene pair was analyzed using the molecular and genetic maps of the *C. reinhardtii* chloroplast genome available from the Chlamydomonas Resource Center (https://www.chlamycollection.org/chloro/genome.html), as well as the genome annotation from GenBank (FJ423446.1) using NCBI Genome Data Viewer (GDV). Four gene pairs displaying a h2h structural organization were identified (Table 2):

Table 2 | Characteristics of putative bidirectional promoters in *C. reinhardtii* chloroplast genome

Putative bidirectional promoters	5' gene	3' gene	Size (bp)	%GC	Numbers CpG	5' gene annotation (function)	3' gene annotation (function)
BDP1	LocACJ 50136	LocACJ 50137	855	58%	2	*RuBisCO large subunit (rbcL)*	*ATP synthase CF1 Alpha subunit (atpA)*
BDP2	LocACJ 50098	LocACJ 500999	632	29%	9	*Cytochrome b6 (petB)*	*Photochloro phyllide reductase subunit L (chiL)*
BDP3	LocACJ 50118	LocACJ 50119	570	30%	8	*Photosystem II reaction center protein H (psbH)*	*Photosystem II reaction center protein N (psbN)*
BDP4	LocACJ 50129	LocACJ 50130	1056	28%	10	*RNA polymerase beta subunit I (rpoB-1)*	*cytochrome b559 beta subunit (PsbF)*

atpA/rbcL, encoding the ATP synthase CF1 α-subunit and the RuBisCO large subunit, separated by an intergenic region (IR) of 855 bp (BDP1, nucleotides 124142–125000); *chlL/petB*, encoding the light-independent protochlorophyllide reductase subunit L and cytochrome b6, separated by 632 bp (BDP2, nucleotides 20,688–21,321); *psbN/psbH*, encoding Photosystem II reaction center proteins N and H, separated by 570 bp (BDP3, nucleotides 77,156–77,725); and *rpoB-1/psbF*, encoding the RNA polymerase β-subunit I and cytochrome b559 β-subunit, separated by 1056 bp (BDP4, nucleotides 101,307–102,362). The corresponding IR sequences were extracted from the *C. reinhardtii* chloroplast genome via NCBI in FASTA format.

The IRs were subsequently screened for core promoter motifs corresponding to the canonical −10 and −35 boxes, recognized by the bacterial-type σ -70 factor and the PEP. To achieve this, we combined a manual strand-specific search with computational promoter prediction using BPROM[47].To assess BDPs IRs conservation across photosynthetic microalgae and higher plants, we examined the structural arrangement of identical gene pairs in the chloroplast genomes of fifteen additional species of microalgae : *Chlamydomonas reinhardtii* (FJ423446.1), *Fusochloris perforata* (KM462882.1), *Botryococcus braunii* (KM462884.1), *Pseudendoclonium akinetum* (AY835431.1), *Koliella corcontica* (KM462874.1), *Interfilum terricola* (KM462881.1), *Chlorella vulgaris* (MT577052.1), *Nephroselmis olivacea* (AF137379.1), *Chloromonas perforata* (KT625416.1), *Volvox carteri* (GU084820), *Dunaliella salina* (GQ250046.1), *Haematococcus pluvialis* (MG677935), *Gonium pectorale* (AP012494), *Eudorina elegans* (MH161344) and *Phaeodactylum tricornutum* (MN937452) and fifteen additional species of higher plants : *Ananas comosus* (NC_026220), *Cannabis sativa* (NC_027223), *Capsicum annuum* (NC_018552), *Catharanthus roseus* (NC_021423), *Curcuma roscoeana* (NC_022928), *Glycine max* (NC_007942), *Gossypium barbadense* (NC_008641), *Nicotiana tabacum* (Z00044), *Oryza sativa* (X15901), *Phaseolus vulgaris* (NC_009259), *Pisum sativum* (NC_014057), *Spinacia oleracea* (NC_002202), *Vanilla planifolia* (NC_026778), *Zea mays* (NC_001666) et *Arabidopsis thaliana* (NC_000932.1). Gene pairs that maintained an h2h configuration across species were considered to be regulated by evolutionarily conserved bidirectional promoters, whereas divergent arrangements suggested non-conserved promoter architecture[34]. Three IRs (BDP1, BDP2, and BDP3) were further selected for bidirectional promoter functional analysis (Table 2; Supplementary Tables 1 and 3). Putative promoter regions (500 bp upstream of the transcripts start site) of the nuclear genes *GPPS, SPPS, FPPS*, and *GGPPS*[86] were extracted from the *C. reinhardtii* nuclear genome (assembly NC_057015.1) using the NCBI Genome Data Viewer. These upstream sequences as well as BDP1 were scanned for cis-regulatory elements associated with MeJA-responsive transcription factors. Specifically, predicted *MYB* and *MYC* binding motifs were identified using the New PLACE database (https://www.dna.affrc.go.jp/PLACE/), which catalogs plant cis-acting regulatory DNA elements[87].

Isolation of the IRs and constructions of chloroplast bidirectional vectors

Chloroplast DNA from *C. reinhardtii* was extracted using the sucrose gradient method[88] and analyzed by electrophoresis on a 0.8% agarose gel. Briefly, a 300 mL, 10-day-old culture of *C. reinhardtii* was harvested at 4000 × g for 5 min, and the resulting pellet was gently resuspended in ice-cold extraction buffer (0.35 M sorbitol, 50 mM Tris–HCl pH 8.0, 5 mM EDTA, 0.1% BSA, 1.5 mM 2-mercaptoethanol). The cell suspension was homogenized on ice and passed through a 100 µm nylon mesh. The filtrate was centrifuged at 200 × g for 15 min at 4 °C to remove nuclei and cell-wall debris, and the resulting supernatant containing intact chloroplasts was collected and centrifuged at 2000 × g for 20 min at 4 °C. The crude chloroplast pellet was resuspended in 5 mL of ice-cold wash buffer (0.35 M sorbitol, 50 mM Tris–HCl pH 8.0, 25 mM EDTA) and carefully layered onto a sucrose step gradient consisting of 9 mL of 52% sucrose overlaid with 3.5 mL of 30% sucrose (prepared in 50 mM Tris–HCl pH 8.0, 25 mM EDTA). The gradient was centrifuged at 1500 × g for 60 min at 4 °C, and the chloroplast band at the 30–52% interface was collected with a wide-bore pipette, diluted twice in 10 mL wash buffer, and centrifuged at 1500 × g for 15 min at 4 °C. The purified chloroplast pellet was resuspended in 2 mL wash buffer and lysed in 4 mL lysis buffer (5% sodium sarcosinate, 50 mM Tris–HCl pH 8.0, 25 mM EDTA), followed by addition of 15 µL Proteinase K (10 mg/mL) and incubation at 55 °C for 4 h. The lysate was cooled on ice for 5 min, mixed with 0.75 mL of 5 M potassium acetate (pH 5.2), chilled for 30 min, and centrifuged at 10,000 × g for 15 min at 4 °C. The supernatant was extracted with equal volumes of saturated phenol and chloroform: isoamyl alcohol (24:1), followed by centrifugation at 10,000 × g for 20 min. DNA was precipitated by adding an equal volume of isopropanol (5 mL) and incubating the mixture overnight at –20 °C. The resulting DNA pellet was washed with 70% ethanol, air-dried, resuspended in 40 µL nuclease-free water, treated with RNase, and assessed for quality and integrity on 0.8% agarose gels (Supplementary Fig. 2a and Supplementary Fig. 3a). The three BDP IRs, together with the *psbA* 3′ untranslated region terminator (T*psbA*/3′ UTR), were amplified from purified chloroplast DNA (Supplementary Fig. 2b and Supplementary Fig. 3b) using PrimeSTAR GXL DNA Polymerase (Takara Bio, Japan) and specific primer pairs (Supplementary Data 1). The reporter genes *mVenus* and *tdTomato* coding sequences were codon-optimized for the *C. reinhardtii* chloroplast genome and synthesized by BIO BASIC (Canada). All constructs were assembled using Gibson Assembly with the NEBuilder® HiFi DNA Assembly Bundle for Large Fragments (New England Biolabs, Canada). Each construct consisted of T*psbA*, *mVenus*, the selected BDP, and *tdTomato*, assembled into three expression fragments T*psbA-mVenus*::*BDP*::*tdTomato*,of 3410, 3187, and 3128 bp, respectively. In all designs, T*psbA* and *mVenus* were positioned in the 3′–5′ orientation relative to the BDP, while *tdTomato* was oriented in the 5′–3′ direction. The 5′ UTRs of *atpA*, *chlL*, and *psbN* were placed upstream of *tdTomato*, while those of *rbcL*, *petB*, and *psbH* were aligned with *mVenus*, maintaining correct orientation and translational frame. The assembled fragments were inserted into the chloroplast expression vector backbone pASapI[52], ensuring the vector's *rbcL* 3′ UTR (T*rbcL*) was fused to *tdTomato* in the correct orientation. The resulting recombinant plasmids were designated pABDP1 (pASapI-*TpsbA-mVenus*::*BDP1*::*tdTomato-TrbcL*), pABDP2, and pABDP3. Constructs were propagated in *E. coli* NEB® 10-beta, and plasmid DNA was purified from 200 mL bacterial cultures using the Geneaid™ Midi Plasmid Kit (Cat. No. PI025). The identity and integrity

of each recombinant plasmid were confirmed by double digestion with XbaI and EcoRI.

To compare the transcriptional strength of natural BDPs with monodirectional counterparts, we constructed control vectors using the well-characterized *psbD*/ 5′ UTR promoter (P*psbD*). The P*psbD* sequence was amplified from *C. reinhardtii* chloroplast DNA (Supplementary Fig. 2c and Supplementary Fig. 3c) using PrimeSTAR GXL DNA Polymerase (Takara Bio, Japan), alongside two fragments, pASapI-*TpsbA-mVenus* and pASapI-*tdTomato-TrbcL*—amplified from the recombinant vector pABDP3 with specific primer sets (Supplementary Data 1). The P*psbD* was subsequently inserted into the *mVenus* and *tdTomato* fragments to generate two monodirectional expression constructs: pAMVe (pASapI-*TpsbA-mVenus-PpsbD*) and pATDt (pASapI-*PpsbD-tdTomato-TrbcL*). The structural integrity of the recombinant plasmids was confirmed by restriction digestion with ScaI and KpnI. All constructs (Supplementary Table 4) were sequenced using Illumina MiSeq technology at the Massachusetts General Hospital Center for Computational and Integrative Biology (MGH CCIB DNA Core, USA) to verify their sequence accuracy before transformation into the *C. reinhardtii* chloroplast (Supplementary Data 2).

C. reinhardtii chloroplast transformation and verification of homoplasmy

Chloroplast transformation was conducted using the biolistic microparticle bombardment method, as previously described[89]. Briefly, microalgae were cultured in liquid TAP medium at 25 °C under dim light conditions (5–10 μmol $m^{-2}s^{-1}$) until reaching a cell density ranging from 8.0×10^5 to 2.0×10^6 cells·mL^{-1}. Subsequently, the cells were harvested by centrifugation at 3000 g for 5 minutes at room temperature and resuspended in fresh TAP medium to a concentration of 2×10^8 cells·mL^{-1}. 300 μL of the resuspended cells were distributed onto freshly prepared selective HSM agar medium and left to dry, uncovered, in a dark, sterile hood for 10 minutes. Approximately 30 mg of microcarriers were washed in 500 μL of absolute ethanol and centrifuged at maximum speed for 1 min at room temperature. To 10 μL of gold microcarriers, 100 μL of 0.05 M spermidine was added and vortexed until the clumps disappeared. Next, 10 μL of plasmid DNA (10 μg, 1 μL/μL) was added to the spermidine-gold mixture and vortexed for 5 s. Subsequently, 100 μL of 1 M $CaCl_2$ was slowly added, and the mixture was allowed to precipitate at room temperature for 10 minutes. The precipitate was resuspended in a Polyvinylpyrrolidone (PVP)/ethanol solution (0.05 mg·mL^{-1} PVP) and transferred to a 15 mL falcon tube. The plasmid DNA coated with gold particles was then bombarded into *C. reinhardtii* chloroplast cells using a Helios gene gun (Bio-Rad Laboratories, Inc., USA). The distance between the plates was maintained between 7 and 12 cm, and a helium pressure of rupture disc was set between 1350 and 1750 psi. Following transformation, the Petri dishes were incubated at 25 °C under dim light overnight, then transferred to constant moderate light (50 μmol $m^{-2}s^{-1}$) and left for approximately 3 to 4 weeks to allow transformed colonies to appear. After 3 to 4 weeks, the colonies were selected and transferred again onto freshly prepared selective HSM agar medium. This streaking process was repeated thrice on selective media before homoplasmy was determined. Colonies were resuspended in 50 μL of 5% Chelex-100 and then heated at 95 °C for 10 min[90]. The mixture was centrifuged at 3500 ×g for 5 minutes at room temperature, and 2 μL of the supernatant was directly used as a template for homoplasmy confirmation through PCR (OneTaq® Quick-Load 2X Master Mix, New England Biolabs, Canada) using a combination of three primers (Supplementary Data 1), and visualization of the amplicons migrated on agarose gels with a ChemiDoc Imaging system (Bio-Rad, Canada).

Total RNA extraction and RT-qPCR for mRNA relative quantification

Six mL of a 5-day-old *C. reinhardtii* culture were harvested and centrifuged at 4000 × g for 5 min in a sterile 15 mL Falcon tube. Total RNA was extracted using Invitrogen TRIzol reagent (Life Technologies, Thermo Fisher Scientific, U.S.A) with minor modifications according to the manufacturer's protocol. These included the addition of NaCl at a final concentration of 100 mM to isopropanol to improve nucleic acid precipitation. RNA samples were treated with TurboDNase (Invitrogen TURBO DNA-free Kit, Thermo Fisher Scientific) following the manufacturer's instructions. RNA yield and quality were assessed by measuring the Abs260/Abs280 ratios using a Nanodrop instrument. Total RNA was then subjected to reverse transcription and qPCR amplification in a single reaction using the Luna Universal One-Step RT-qPCR kit (New England Biolabs, Canada). Primers for *mVenus* and *tdTomato* transcripts were designed using the PrimerQuest™ Tool (IDT) (Supplementary Data 1). SYBR Green fluorescence was recorded in the FAM channel of a CFX Connect real-time PCR system (Bio-Rad). PCR analyses were conducted using Bio-Rad CFX Manager version 3.1 software, and relative mRNA expression levels were calculated using the $2^{(-\Delta Ct)}$ method with *GBLP* (β-subunit-like protein) and *histone3* as reference transcripts. The experiments were performed using three biological replicates.

Fluorescence assessment and localization

For flow cytometry analysis, transformants were cultured in liquid TAP medium in sterile 24-well microplates and incubated in a growth chamber at 25 °C, with shaking at 131 rpm, under moderate light conditions (50–60 μmol m^{-2} s^{-1}) for 5 or 13 days. After incubation, 70 μL of the cultures were filtered and transferred into sterile 96-well plates containing 200 μL of TAP medium for fluorescent measurement. The percentage of fluorescent cells and the mean fluorescence intensity per cell were quantified using a CytoFLEX S flow cytometer (Beckman Colter Life Sciences, U.S.A) equipped with violet (405 nm), blue (488 nm), yellow green (561 nm), and red (638 nm) lasers. Cells were gated based on forward scatter area (FSC-A) and side scatter area (SSC-A) parameters. Chlorophyll autofluorescence was detected in the PerCP channel (690/50 nm), excluding non-specific autofluorescence in the PB450 channel (450/45 nm). mVenus fluorescence was analyzed in the FITC channel (524/40 nm), while tdTomato fluorescence was detected in the PE channel (585/42 nm BP). For tdTomato positive control, the CC4388 strain was treated with 10% DMSO and propidium iodide (PI). Briefly, 1 mL of culture grown in liquid TAP medium at 25 °C, under dim light (5–10 μmol m^{-2} s^{-1}) and shaking at 131 rpm, was harvested.centrifuged (3000 × g, 5 min), and the cell pellet was resuspended in 1 mL TAP. A working solution was prepared to obtain final concentrations of 5 μg/mL PI and 10% (v/v) DMSO. The mixture (900 μL cell suspension + 100 μL DMSO solution containing PI) was incubated for 10 min at room temperature in the dark. After incubation, the cells were used directly for flow cytometry analysis. Data analysis was conducted using BD FlowJo version 10 software (BD Biosciences, La Jolla, CA, U.S.A, 2020). The subcellular localization of mVenus and tdTomato fluorescent proteins was visualized using a Leica TCS SP8 confocal laser scanning microscope (Wetzlar, Hesse, Germany), and the images were merged using ImageJ software (V1.8.0).

Growth curves (OD_{750}, 750/8 nm), chlorophyll (excitation 475/18 nm, emission 650/18 nm), mVenus (excitation 500/18 nm, emission 541/18 nm), and tdTomato fluorescence were obtained over 13 days using a Synergy H4 Gen5 2.07 microplate reader (Biotek, Agilent) from three biological replicates for each transplastomic cell line. Cells were inoculated into 50 mL of fresh TAP medium in sterile 125 mL Erlenmeyer flasks and incubated in a growth chamber (50–60 μmol photons $m^{-2}s^{-1}$, 25 °C, and 131 rpm). 300 μL of cell culture was transferred to a 96-Well plate for fluorescence measurement.

For methyl jasmonate (MeJA) treatment, transplastomic cell lines were inoculated in fresh TAP medium at a cell density of approximately 1×10^4 cells·mL^{-1} (OD_{750nm} = 0.01) in triplicates in 96-well flat-bottom microplates (Corning Costar 96-Well, Cell Culture-Treated, Fisher Scientific). The cultures were incubated in a growth chamber at 25 °C, with shaking at 131 rpm, under moderate light conditions (50–60 μmol m^{-2} s^{-1}) for eight days. MeJa (0.5 mM final concentration) was added to the medium at the

mid-exponential growth phase (day 4) to induce transgenes accumulation. The fluorescence intensity of mVenus and tdTomato was measured over eight days and normalized to chlorophyll content, while mRNA levels were measured after 24 h of induction.

Whole-cell extract and western blot analysis

Cells from liquid culture were collected by centrifugation at 4000 × g for 5 min. Whole-cell extracts were prepared by resuspending the cellular pellets (normalized by OD_{750nm}) in 1X Laemmli buffer containing 1% β-mercaptoethanol (v/v) and boiling at 95 °C for 5 min. The samples were then centrifuged at 16,000 × g for 2 minutes, and the supernatant was loaded onto a 10% SDS-PAGE gel. Proteins were transferred to a membrane using a Trans-Blot SD semi-dry transfer cell (Bio-Rad). mVenus protein was detected using an anti-GFP/CFP/YFP Tag primary antibody[91], purified (Clone 1218) (Mouse IgG1), supplied by Cedarlane (Product Code: CLH106AP) at a 1:2000 dilution. Each immunoblot experiment was conducted at least twice, with an empty vector (EV) serving as a negative control and a strain C21 expressing nuclear mVenus used as a positive control.

Statistics and reproducibility

For RT-qPCR and methyl jasmonate (MeJA) induction experiments, data were collected from at least three independent biological replicates ($n = 3$), each corresponding to distinct transplastomic *C. reinhardtii* cultures transformed with different promoter constructs. For flow cytometry (FACS) analyses, data were obtained from a minimum of six independent transplastomic cell lines ($n \geq 6$). Measurements were performed on independent biological samples rather than repeated measures from the same culture, except where explicitly stated (time-course experiments). Statistical analyses were conducted using GraphPad Prism (version 8.1.2) and FlowJo v10.7.1 for FACS data. Data are presented as mean ± standard deviation (sd). Normality of the datasets was assessed using the Shapiro–Wilk test. Comparisons between two groups were performed using unpaired two-tailed Student's t-tests, with $p < 0.05$ considered statistically significant. Exact *p*-values are reported in the figure legends or within the main text. Figures were generated using GraphPad Prism v8.1.2, FlowJo v10.7.1, BioRender.com, and RStudio v4.3.0.

Reporting summary

Further information on research design is available in the Nature Portfolio Reporting Summary linked to this article.

Data availability

All data supporting the findings of this study are included in the main text and Supplementary Information. Oligonucleotide sequences are listed in Supplementary Data 1. Next-generation sequencing (NGS) results for all plasmid constructs are provided in Supplementary Data 2. Flow cytometry, RT–qPCR, and confocal microscopy datasets are available in Supplementary Data 3. Raw NGS reads have been deposited in the NCBI Sequence Read Archive under BioProject accession number PRJNA1379576. The plasmid vectors pABDP1, pABDP2, pABDP3, pAMVe, and pATDt have been deposited in Addgene under accession numbers 249500, 249501, 249502, 249494, and 249499, respectively.

Received: 20 May 2025; Accepted: 23 December 2025;
Published online: 03 January 2026

References

1. Kumar, G. et al. Bioengineering of microalgae: recent advances, perspectives, and regulatory challenges for industrial application. *Front. Bioeng. Biotechnol.* **8**, 914 (2020).
2. Rasala, B. A. & Mayfield, S. P. The microalga Chlamydomonas reinhardtii as a platform for the production of human protein therapeutics. *Bioeng. Bugs* **2**, 50–54 (2011).
3. Harris, E. H. Chlamydomonas as a model organism. *Annu. Rev. Plant Physiol. Plant Mol. Biol.* **52**, 363–406 (2001).
4. Fabris, M. et al. Emerging technologies in algal biotechnology: toward the establishment of a sustainable, algae-based bioeconomy. *Front. Plant Sci.* **11**, 279 (2020).
5. Taunt, H. N., Stoffels, L. & Purton, S. Green biologics: the algal chloroplast as a platform for making biopharmaceuticals. *Bioengineered* **9**, 48–54 (2018).
6. Neupert, J. et al. An epigenetic gene silencing pathway selectively acting on transgenic DNA in the green alga Chlamydomonas. *Nat. Commun.* **11**, 6269 (2020).
7. Purton, S. Tools and techniques for chloroplast transformation of Chlamydomonas. *Adv. Exp. Med Biol.* **616**, 34–45 (2007).
8. Ramesh, V. M., Bingham, S. E. & Webber, A. N. A simple method for chloroplast transformation in Chlamydomonas reinhardtii. *Methods Mol. Biol.* **684**, 313–320 (2011).
9. Mordaka, P. M. et al. Regulation of nucleus-encoded trans-acting factors allows orthogonal fine-tuning of multiple transgenes in the chloroplast of Chlamydomonas reinhardtii. *Plant Biotechnol J* **n/a** (2024). https://doi.org/10.1111/pbi.14557
10. Larrea-Alvarez, M. & Purton, S. Multigenic engineering of the chloroplast genome in the green alga Chlamydomonas reinhardtii. *Microbiology* **166**, 510–515 (2020).
11. Yeon, J., Miller, S. M. & Dejtisakdi, W. New synthetic operon vectors for expressing multiple proteins in the chlamydomonas reinhardtii chloroplast. *Genes* **14**, 368 (2023).
12. Macedo-Osorio, K. S. et al. Intercistronic expression elements (IEE) from the chloroplast of Chlamydomonas reinhardtii can be used for the expression of foreign genes in synthetic operons. *Plant Mol. Biol.* **98**, 303–317 (2018).
13. Guo, Y., Xiong, H., Fan, Q. & Duanmu, D. Heterologous gene expression in chlamydomonas reinhardtii chloroplast by heterologous promoters and terminators, intercistronic expression elements and minichromosome. *Micro. Biotechnol.* **17**, e70069 (2024).
14. Melero-Cobo, X. et al. MoCloro: an extension of the Chlamydomonas reinhardtii modular cloning toolkit for microalgal chloroplast engineering. *Physiol. Plant* **177**, e70088 (2025).
15. Inckemann, R. M. et al. A modular high-throughput approach for advancing synthetic biology in the chloroplast of Chlamydomonas. *Nat, Plants* (2025). https://doi.org/10.1038/s41477-025-02126-2
16. Zhang, P. et al. Deep flanking sequence engineering for efficient promoter design using DeepSEED. *Nat. Commun.* **14**, 6309 (2023).
17. Altendorfer, E., Mundlos, S. & Mayer, A. A transcription coupling model for how enhancers communicate with their target genes. *Nat. Struct. Mol. Biol.* **32**, 598–606 (2025).
18. Johnson, C. H. & Schmidt, G. W. The psbB gene cluster of the Chlamydomonas reinhardtii chloroplast: sequence and transcriptional analyses of psbN and psbH. *Plant Mol. Biol.* **22**, 645–658 (1993).
19. Stern, D. S., Higgs, D. C. & Yang, J. Transcription and translation in chloroplasts. *Trends Plant Sci.* **2**, 308–315 (1997).
20. Klein, U., De Camp, J. D. & Bogorad, L. Two types of chloroplast gene promoters in Chlamydomonas reinhardtii. *Proc. Natl. Acad. Sci. USA* **89**, 3453–3457 (1992).
21. Hatano-Iwasaki, A., Minagawa, J., Inoue, Y. & Takahashi, Y. Characterization of chloroplast psbA transformants of Chlamydomonas reinhardtii with impaired processing of a precursor of a photosystem II reaction center protein, D1. *Plant Mol. Biol.* **42**, 353–363 (2000).
22. Rasala, B. A., Muto, M., Sullivan, J. & Mayfield, S. P. Improved heterologous protein expression in the chloroplast of Chlamydomonas reinhardtii through promoter and 5' untranslated region optimization. *Plant Biotechnol. J.* **9**, 674–683 (2011).
23. Drapier, D. et al. The chloroplast atpA gene cluster in Chlamydomonas reinhardtii. Functional analysis of a polycistronic transcription unit. *Plant Physiol.* **117**, 629–641 (1998).

24. Shimmura, S. et al. Comparative analysis of chloroplast psbD promoters in terrestrial plants. *Front Plant Sci.* **8**, 1186 (2017).
25. Nickelsen, J., Fleischmann, M., Boudreau, E., Rahire, M. & Rochaix, J.-D. Identification of cis-Acting RNA leader elements required for chloroplast psbD gene expression in chlamydomonas. *Plant Cell* **11**, 957–970 (1999).
26. Klein, U., Salvador, M. L. & Bogorad, L. Activity of the Chlamydomonas chloroplast RBCL gene promoter is enhanced by a remote sequence element. *Proc. Natl. Acad. Sci.* **91**, 10819–10823 (1994).
27. Scranton, M. A., Ostrand, J. T., Fields, F. J. & Mayfield, S. P. Chlamydomonas as a model for biofuels and bio-products production. *Plant J.* **82**, 523–531 (2015).
28. Anthonisen, I. L., Salvador, M. L. & Klein, U. Specific sequence elements in the 5' untranslated regions of rbcL and atpB gene mRNas stabilize transcripts in the chloroplast of Chlamydomonas reinhardtii. *RNA* **7**, 1024–1033 (2001).
29. Cavaiuolo, M., Kuras, R., Wollman, F. A., Choquet, Y. Vallon, O. Small RNA profiling in Chlamydomonas: insights into chloroplast RNA metabolism. *Nucleic Acids Res.* **45**, 10783–10799 (2017).
30. Loiselay, C. et al. Molecular identification and function of cis- and trans-acting determinants for petA transcript stability in Chlamydomonas reinhardtii chloroplasts. *Mol. Cell Biol.* **28**, 5529–5542 (2008).
31. Johnson, X. et al. MRL1, a conserved Pentatricopeptide repeat protein, is required for stabilization of rbcL mRNA in chlamydomonas and arabidopsis. *Plant Cell* **22**, 234–248 (2010).
32. Boudreau, E., Nickelsen, J., Lemaire, S. D., Ossenbühl, F. & Rochaix, J. D. The Nac2 gene of Chlamydomonas encodes a chloroplast TPR-like protein involved in psbD mRNA stability. *Embo J.* **19**, 3366–3376 (2000).
33. Commault, A. S. et al. Methyl jasmonate treatment affects the regulation of the 2-C-methyl-D-erythritol 4-phosphate pathway and early steps of the triterpenoid biosynthesis in Chlamydomonas reinhardtii. *Algal Res.* **39**, 101462 (2019).
34. Wang, R. et al. Isolation and functional characterization of bidirectional promoters in rice. *Front Plant Sci.* **7**, 766 (2016).
35. In, S., Lee, H. A., Woo, J., Park, E. & Choi, D. Molecular characterization of a pathogen-inducible bidirectional promoter from hot pepper (Capsicum annuum). *Mol. Plant Microbe Interact.* **33**, 1330–1339 (2020).
36. Liu, X. et al. The intergenic region of the maize defensin-like protein genes Def1 and Def2 functions as an embryo-specific asymmetric bidirectional promoter. *J. Exp. Bot.* **67**, 4403–4413 (2016).
37. Thieffry, A. et al. Characterization of arabidopsis thaliana promoter bidirectionality and antisense RNAs by inactivation of nuclear RNA decay pathways. *Plant Cell* **32**, 1845–1867 (2020).
38. Vogl, T. et al. Engineered bidirectional promoters enable rapid multi-gene co-expression optimization. *Nat. Commun.* **9**, 3589 (2018).
39. Yang, S., Sleight, S. C. & Sauro, H. M. Rationally designed bidirectional promoter improves the evolutionary stability of synthetic genetic circuits. *Nucleic Acids Res.* **41**, e33 (2013).
40. Kumar, S. et al. A combinatorial bidirectional and bicistronic approach for coordinated multi-gene expression in corn. *Plant Mol. Biol.* **87**, 341–353 (2015).
41. Poliner, E., Clark, E., Cummings, C., Benning, C. & Farre, E. M. A high-capacity gene stacking toolkit for the oleaginous microalga, Nannochloropsis oceanica CCMP1779. *Algal Res.* **45**, 101664 (2020).
42. Büschlen, S., Choquet, Y., Kuras, R. & Wollman, F.-A. Nucleotide sequences of the continuous and separated petA, petB and petD chloroplast genes in Chlamydomonas reinhardtii. *FEBS Lett.* **284**, 257–262 (1991).
43. Sakamoto, W., Chen, X., Kindle, K. L. & Stern, D. B. Function of the Chlamydomonas reinhardtii petd 5' untranslated region in regulating the accumulation of subunit IV of the cytochrome b6/f complex. *Plant J.* **6**, 503–512 (1994).
44. Loizeau, K. et al. Small RNAs reveal two target sites of the RNA-maturation factor Mbb1 in the chloroplast of Chlamydomonas. *Nucleic Acids Res.* **42**, 3286–3297 (2013).
45. Fong, S. E. & Surzycki, S. J. Organization and structure of plastome psbF, psbL, petG and ORF712 genes in Chlamydomonas reinhardtii. *Curr. Genet.* **21**, 527–530 (1992).
46. Fong, S. E. & Surzycki, S. J. Chloroplast RNA polymerase genes of Chlamydomonas reinhardtii exhibit an unusual structure and arrangement. *Curr. Genet* **21**, 485–497 (1992).
47. Solovyev, V. V. & Salamov, A. A. Recognition of 3'-processing sites of human mRNA precursors. *Comput. Appl. Biosci.* **13**, 23–28 (1997).
48. Ma, K., Deng, L., Wu, H. & Fan, J. Towards green biomanufacturing of high-value recombinant proteins using promising cell factory: chlamydomonas reinhardtii chloroplast. *Bioresour. Bioprocess* **9**, 83 (2022).
49. Miro-Vinyals, B. et al. Chloroplast engineering of the green microalgae Chlamydomonas reinhardtii for the production of HAA, the lipid moiety of rhamnolipid biosurfactants. *N. Biotechnol.* **76**, 1–12 (2023).
50. Di Rocco, G. et al. A PETase enzyme synthesised in the chloroplast of the microalga Chlamydomonas reinhardtii is active against post-consumer plastics. *Sci. Rep.* **13**, 10028 (2023).
51. Barnes, D. et al. Contribution of 5'- and 3'-untranslated regions of plastid mRNAs to the expression of Chlamydomonas reinhardtii chloroplast genes. *Mol. Genet Genomics* **274**, 625–636 (2005).
52. Economou, C., Wannathong, T., Szaub, J. & Purton, S. A simple, low-cost method for chloroplast transformation of the green alga Chlamydomonas reinhardtii. *Methods Mol. Biol.* **1132**, 401–411 (2014).
53. Nishimura, Y. & Stern, D. B. Differential replication of two chloroplast genome forms in heteroplasmic Chlamydomonas reinhardtii gametes contributes to alternative inheritance patterns. *Genetics* **185**, 1167–1181 (2010).
54. Khan, A. et al. Plant synthetic promoters: advancement and prospective. *Agriculture* **13**, 298 (2023).
55. Anwar, M., Wang, J., Li, J., Altaf, M. M. & Hu, Z. MYB transcriptional factors affects upstream and downstream MEP pathway and triterpenoid biosynthesis in chlamydomonas reinhardtii. *Processes* **12**, 487 (2024).
56. Wasternack, C. & Hause, B. Jasmonates: biosynthesis, perception, signal transduction and action in plant stress response, growth and development. An update to the 2007 review in Annals of Botany. *Ann. Bot.* **111**, 1021–1058 (2013).
57. Goossens, J., Fernandez-Calvo, P., Schweizer, F. & Goossens, A. Jasmonates: signal transduction components and their roles in environmental stress responses. *Plant Mol. Biol.* **91**, 673–689 (2016).
58. Al Hoqani, U. H. A. Metabolic engineering of the algal chloroplast for terpenoid production. *Doctoral thesis*, UCL (University College London) (2017).
59. Wichmann, J. et al. Farnesyl pyrophosphate compartmentalization in the green microalga Chlamydomonas reinhardtii during heterologous (E)-alpha-bisabolene production. *Micro. Cell Fact.* **21**, 190 (2022).
60. Pérez-Martín, J. & de Lorenzo, V. Clues and consequences of DNA bending in transcription. *Annu. Rev. Microbiol.* **51**, 593–628 (1997).
61. Summer, E. J., Schmid, V. H., Bruns, B. U. & Schmidt, G. W. Requirement for the H phosphoprotein in photosystem II of Chlamydomonas reinhardtii. *Plant Physiol.* **113**, 1359–1368 (1997).
62. Torabi, S. et al. PsbN is required for assembly of the photosystem II reaction center in Nicotiana tabacum. *Plant Cell* **26**, 1183–1199 (2014).
63. Rosales-Mendoza, S., Paz-Maldonado, L. M. T. & Soria-Guerra, R. E. Chlamydomonas reinhardtii as a viable platform for the production of recombinant proteins: current status and perspectives. *Plant Cell Rep.* **31**, 479–494 (2012).
64. Surzycki, R. et al. Factors effecting expression of vaccines in microalgae. *Biologicals* **37**, 133–138 (2009).

65. Barnes, D. et al. Contribution of 5′- and 3′-untranslated regions of plastid mRNAs to the expression of Chlamydomonas reinhardtii chloroplast genes. *Mol. Genet. Genomics* **274**, 625–636 (2005).
66. Wannathong, T., Waterhouse, J. C., Young, R. E., Economou, C. K. & Purton, S. New tools for chloroplast genetic engineering allow the synthesis of human growth hormone in the green alga Chlamydomonas reinhardtii. *Appl Microbiol Biotechnol.* **100**, 5467–5477 (2016).
67. Odom, O. W., Kang, S., Ferguson, C., Chen, C. & Herrin, D. L. Overcoming poor transgene expression in the wild-type chlamydomonas chloroplast: creation of highly mosquitocidal strains of chlamydomonas reinhardtii. *Microorganisms* **10**, 1087 (2022).
68. Coragliotti, A. T., Beligni, M. V., Franklin, S. E. & Mayfield, S. P. Molecular factors affecting the accumulation of recombinant proteins in the Chlamydomonas reinhardtii chloroplast. *Mol. Biotechnol.* **48**, 60–75 (2011).
69. Barkan, A. Expression of plastid genes: organelle-specific elaborations on a prokaryotic scaffold. *Plant Physiol.* **155**, 1520–1532 (2011).
70. Kasai, S. et al. Effect of coding regions on chloroplast gene expression in Chlamydomonas reinhardtii. *J. Biosci. Bioeng.* **95**, 276–282 (2003).
71. Kato, K., Ishikura, K., Kasai, S. & Shinmyo, A. Efficient translation destabilizes transcripts in chloroplasts of Chlamydomonas reinhardtii. *J. Biosci. Bioeng.* **101**, 471–477 (2006).
72. Viola, S. et al. MDA1, a nucleus-encoded factor involved in the stabilization and processing of the atpA transcript in the chloroplast of Chlamydomonas. *Plant J.* **98**, 1033–1047 (2019).
73. Eberhard, S. et al. Dual functions of the nucleus-encoded factor TDA1 in trapping and translation activation of atpA transcripts in Chlamydomonas reinhardtii chloroplasts. *Plant J.* **67**, 1055–1066 (2011).
74. Chaux, F. et al. Chloroplast ATP synthase biogenesis requires peripheral stalk subunits AtpF and ATPG and stabilization of atpE mRNA by OPR protein MDE1. *Plant J.* **116**, 1582–1599 (2023).
75. Anthonisen, I. L., Salvador, M. L. & Klein, U. W. E. Specific sequence elements in the 5′ untranslated regions of rbcL and atpB gene mRNAs stabilize transcripts in the chloroplast of Chlamydomonas reinhardtii. *RNA* **7**, 1024–1033 (2001).
76. Hauser, C. R., Gillham, N. W. & Boynton, J. E. Translational regulation of chloroplast genes: proteins binding to the 5′-untranslated regions of chloroplast mrnas in chlamydomonas reinhardtii(∗). *J. Biol. Chem.* **271**, 1486–1497 (1996).
77. Odom, O. W., Kang, S., Ferguson, C., Chen, C. & Herrin, D. L. Overcoming poor transgene expression in the wild-type chlamydomonas chloroplast: creation of highly mosquitocidal strains of chlamydomonas reinhardtii. *Microorganisms* **10** (2022). https://doi.org/10.3390/microorganisms10061087
78. Miró-Vinyals, B. et al. Chloroplast engineering of the green microalgae Chlamydomonas reinhardtii for the production of HAA, the lipid moiety of rhamnolipid biosurfactants. *N. Biotechnol.* **76**, 1–12 (2023).
79. Mordaka, P. M. et al. Regulation of nucleus-encoded trans-acting factors allows orthogonal fine-tuning of multiple transgenes in the chloroplast of Chlamydomonas reinhardtii. *Plant Biotechnol. J.* **23**, 1005–1018 (2025).
80. Kurowska, M. M. et al. Methyl Jasmonate Affects Photosynthesis Efficiency, Expression of HvTIP Genes and Nitrogen Homeostasis in Barley. *Int J Mol Sci* **21** (2020). https://doi.org/10.3390/ijms21124335
81. Xie, D. X., Feys, B. F., James, S., Nieto-Rostro, M. & Turner, J. G. COI1: an Arabidopsis gene required for jasmonate-regulated defense and fertility. *Science* **280**, 1091–1094 (1998).
82. Devoto, A. et al. COI1 links jasmonate signalling and fertility to the SCF ubiquitin-ligase complex in Arabidopsis. *Plant J.* **32**, 457–466 (2002).
83. Chini, A., Boter, M. & Solano, R. Plant oxylipins: COI1/JAZs/MYC2 as the core jasmonic acid-signalling module. *FEBS J.* **276**, 4682–4692 (2009).
84. Staswick, P. E. JAZing up jasmonate signaling. *Trends Plant Sci.* **13**, 66–71 (2008).
85. Fonseca, S., Chico, J. M. & Solano, R. The jasmonate pathway: the ligand, the receptor and the core signalling module. *Curr. Opin. Plant Biol.* **12**, 539–547 (2009).
86. Lohr, M., Schwender, J. & Polle, J. E. Isoprenoid biosynthesis in eukaryotic phototrophs: a spotlight on algae. *Plant Sci.* **185-186**, 9–22 (2012).
87. Higo, K., Ugawa, Y., Iwamoto, M. & Higo, H. PLACE: a database of plant cis-acting regulatory DNA elements. *Nucleic Acids Res*. **26**, 358–359 (1998).
88. Jansen, R. K. et al. Methods for obtaining and analyzing whole chloroplast genome sequences. *Methods Enzymol.* **395**, 348–384 (2005).
89. Barrera, D., Gimpel, J. & Mayfield, S. in *Chloroplast Biotechnology: Methods and Protocols* (ed Pal Maliga) 391-399 (Humana Press, 2014).
90. Nouemssi, S. B. et al. Rapid and efficient colony-pcr for high throughput screening of genetically transformed chlamydomonas reinhardtii. *Life* **10**, 186 (2020).
91. Nagai, T. et al. A variant of yellow fluorescent protein with fast and efficient maturation for cell-biological applications. *Nat. Biotechnol.* **20**, 87–90 (2002).

Acknowledgements

The authors thank Dr. Karen Cristine Goncalves dos Santos for her valuable technical advice and input during this study, and Melodie B. Plourde for her generous support and patience in assisting with confocal microscopy acquisition and analysis. During the preparation of this work, the authors used ChatGPT -4.0, a free AI language model, to correct grammatical errors and enhance readability. After using this tool, the authors reviewed and edited the content as needed and take full responsibility for the final version of this publication. This research was funded by Canada Research Chair on plant specialized metabolism Award No. CRC-2023 00353 to IDP. The authors extent their gratitude to the Canadian taxpayers and to the Canadian government for supporting the Canada Research Chairs Program. Additional funding was provided by the Natural Sciences and Engineering Research Council of Canada (NSERC) through award No. RGPIN/3218-2021 to IDP. This work was also supported by NSERC award No. EQPEQ 472990-2015 (Research tools and instruments program) for the acquisition of the qPCR system.

Author contributions

A.W.T.: Conceptualization, Formal analysis, Investigation, Methodology, Validation, Visualization, Writing-Original draft, Writing Reviewing and Editing; N.M.: Conceptualization, Formal analysis, Methodology, Project administration Supervision, Writing-Original draft, Writing Reviewing and Editing; E.F.: Formal analysis, Investigation, Methodology, Writing Reviewing and Editing; A.B.: Investigation, Methodology, Writing Reviewing and Editing; F.A.: Investigation, Writing Reviewing and Editing; F.M.-M.: Conceptualization, Methodology, Project administration, Writing Reviewing and Editing; I.D.P.: Conceptualization, Funding, acquisition, Methodology, Project administration, Resources, Supervision, Validation, Writing- Reviewing and Editing.

Competing interests

The authors declare no competing interests.

Additional information

Supplementary information The online version contains supplementary material available at https://doi.org/10.1038/s42003-025-09478-7.

Correspondence and requests for materials should be addressed to Isabel Desgagné-Penix.

Peer review information *Communications Biology* thanks Bradley W. Abramson, Frédéric Chaux and Domitille Jarrige for their contribution to the peer review of this work. Primary Handling Editors: Leena Tripathi, George Inglis, and David Favero.